AN ANALYSIS OF SIMULATED CALIFORNIA CLIMATE USING MULTIPLE DYNAMICAL AND STATISTICAL TECHNIQUES

A Paper From:
California Climate Change Center

Prepared By:
N. L. Miller[1,2], J. Jin[1,3], N. J. Schlegel [1,2], M. A. Snyder[4], T.O'Brien[4], L. C. Sloan[4], P.B. Duffy[5], H. Hidalgo[6], Kanamaru[6], M. Kanamitsu[6], K. Yoshimura[6], D.R. Cayan[6,7]

[1]Lawrence Berkeley National Laboratory; [2]University of California, Berkeley; [3]Utah State University, [4]University of California Santa Cruz; [5]Lawrence Livermore National Laboratory; [6]University of California San Diego; [7]US Geological Survey

DRAFT PAPER

DISCLAIMER

This paper was prepared as the result of work sponsored by the California Energy Commission (Energy Commission) and the California Environmental Protection Agency (Cal/EPA). It does not necessarily represent the views of the Energy Commission, Cal/EPA, their employees, or the State of California. The Energy Commission, Cal/EPA, the State of California, their employees, contractors, and subcontractors make no warrant, express or implied, and assume no legal liability for the information in this paper; nor does any party represent that the uses of this information will not infringe upon privately owned rights. This paper has not been approved or disapproved by the California Energy Commission or Cal/EPA, nor has the California Energy Commission or Cal/EPA passed upon the accuracy or adequacy of the information in this paper.

Arnold Schwarzenegger, *Governor*

March 2009
CEC-500-2009-017-D

Acknowledgments

Support for this work was provided by the California Energy Commission's Public Interest Energy Research (PIER) Program under the Climate Change subprogram. Work performed at Lawrence Berkeley National Laboratory and Lawrence Livermore National Laboratory is under the auspices of the U.S. Department of Energy under contract DE-AC03-76F00098 and W-7405-Eng-48, respectively, with funding provided by the Energy Commission. Model simulations performed by Masao Kanamitsu, Hideki Kanamaru, Kei Yoshimura using the Regional Spectral Model (RSM); Mark Snyder, Travis O'Brien, and Lisa Sloan using the Regional Climate Model (RegCM); Jiming Jin, Nicole Schlegel, and Norman Miller using the Weather, Research, and Forecasting-Community Land Model (WRF-CLM) and Weather, Research, and Forecasting-Rapid Update Cycle (WRF-RUC); and Hugo Hidalgo and Daniel R. Cayan using the Constructed Analogues statistical model (CANA).

Preface

The California Energy Commission's Public Interest Energy Research (PIER) Program supports public interest energy research and development that will help improve the quality of life in California by bringing environmentally safe, affordable, and reliable energy services and products to the marketplace.

The PIER Program conducts public interest research, development, and demonstration (RD&D) projects to benefit California's electricity and natural gas ratepayers. The PIER Program strives to conduct the most promising public interest energy research by partnering with RD&D entities, including individuals, businesses, utilities, and public or private research institutions.

PIER funding efforts focus on the following RD&D program areas:

- Buildings End-Use Energy Efficiency
- Energy-Related Environmental Research
- Energy Systems Integration
- Environmentally Preferred Advanced Generation
- Industrial/Agricultural/Water End-Use Energy Efficiency
- Renewable Energy Technologies
- Transportation

In 2003, the California Energy Commission's PIER Program established the **California Climate Change Center** to document climate change research relevant to the states. This center is a virtual organization with core research activities at Scripps Institution of Oceanography and the University of California, Berkeley, complemented by efforts at other research institutions. Priority research areas defined in PIER's five-year Climate Change Research Plan are: monitoring, analysis, and modeling of climate; analysis of options to reduce greenhouse gas emissions; assessment of physical impacts and of adaptation strategies; and analysis of the economic consequences of both climate change impacts and the efforts designed to reduce emissions.

The California Climate Change Center Report Series details ongoing center-sponsored research. As interim project results, the information contained in these reports may change; authors should be contacted for the most recent project results. By providing ready access to this timely research, the center seeks to inform the public and expand dissemination of climate change information, thereby leveraging collaborative efforts and increasing the benefits of this research to California's citizens, environment, and economy.

For more information on the PIER Program, please visit the Energy Commission's website www.energy.ca.gov/pier/ or contract the Energy Commission at (916) 654-5164.

Table of Contents

Preface iii
Abstract ix
Executive Summary 1
1.0 Introduction 2
2.0 Approach 4
2.1. Dynamic and Statistical Downscaling 5
2.2. Input Data 8
3.0 Results 9
3.1. Climatological Means of Temperature and Precipitation 10
3.2. Snow Water Equivalent 15
3.3. Spatio-Temporal Variability 17
3.4. Surface Energy Fluxes 18
3.5. Geopotential Heights and Surface Winds 22
4.0 Summary and Conclusions 28
5.0 References 29

List of Figures

Figure 1. Model domains used in this study. A. Western United States and Eastern Pacific Ocean, 30 km resolution, [139W21N x 104W51N], B. California, Nevada, Eastern Pacific Ocean, 10 km resolution, [128W31N x 113W44N]..... 5

Figure 2. Climatological (1980–1989) differences between the PRISM and NARR for (A) NDJFM precipitation, (B) DJF Tmax, (C) JJA Tmax, and (D) JJA Tmin 9

Figure 3a. Seasonal mean of daily maximum 2 m air temperature during June–August. Results shown are climatological means for 1980–1989. 11

Figure 3b. Like Figure 3a, except for JJA daily minimum temperatures. 11

Figure 4a. Seasonal mean of daily maximum 2 m air temperature during December–February 13

Figure 4b. Like Figure 4a, except for DJF daily minimum temperatures..... 13

Figure 5a. Cumulative November–March precipitation, climatological mean for 1980–1989..... 14

Figure 5b. Cumulative November–March precipitation differences relative to PRISM..... 14

Figure 5c. Temporal correlations between monthly mean precipitation in models and the PRISM observation-based data set, based on the climatological mean for 1980–1989..... 15

Figure 6. Top: Spatial mean Snow Water Equivalent (SWE) in a Sierra Nevada subdomain for WRF-CLM, WRF-RUC, and RegCM3 with COOP observations. 16

Figure 7. Taylor diagrams showing WRF-CLM3, WRF-RUC, RSM, and RegCM model-to-observation performance scores based on normalized standard deviations and correlations for monthly means of (a) maximum temperature, (b) minimum temperature, (c) precipitation, and (d) SWE..... 18

Figure 8. Regcm3, RSM, WRF-CLM, and the North American Regional Reanalysis (NARR) climatological (1980–1989) surface latent heat fluxes. for (A) DJF and (B) JJA 19

Figure 9. Regcm3, RSM, WRF-CLM, and the North American Regional Reanalysis (NARR) climatological (1980–1989) surface sensible heat fluxes for (A) DJF and (B) JJA 20

Figure 10. Same as Figure 9, except showing upwelling solar radiation at the surface..... 21

Figure 11. Same as Figure 10, except showing *downwelling longwave* radiation at the surface 22

Figure 12. Geopotential height (a) January mean-monthly distribution, and (b) July mean-monthly distribution..... 23

Figure 13. Model and Reanalysis comparison of the 500 hectopascal (hPa) geopotential height for three locations P1. 120W, 39N (American River Basin), P2. 117.5W, 37N (Merced Basin), and P3. 122.5W, 38N (Russian River Basin) 24

Figure 14. Model and reanalysis near-surface wind speed and direction for (a) mean-October 1982 and (b) mean-January 1983 25

Figure 15. Hovmueller plots of the JJA wind speed and direction across latitude 38.5N. The legend along the bottom is wind speed in meters per second. 26

Figure 16. Hovmueller plots of the winter precipitation across latitude 38.5N 27

List of Tables

Table 1. Summary of RCM settings 7

Abstract

Four dynamic regional climate models (University of California, Santa Cruz's RegCM3; the University of California, San Diego's RSM; the National Center for Atmospheric Research's WRF-RUC; and the Lawrence Berkeley National Laboratory/University of California, Berkeley's WRF-CLM3) and one statistical downscaling approach (the University of California, San Diego's CANA) were used to downscale 10 years of historical climate in California. To isolate possible limitations of the downscaling methods, initial and lateral boundary conditions from the National Centers for Environmental Prediction global reanalysis were used. Results of this downscaling were compared to observations and to an independent, fine-resolution reanalysis (the North American Regional Reanalysis). This evaluation is preparation for simulations of future-climate scenarios, the second phase of this California Energy Commission climate projections project, *which will lead to probabilistic scenarios*. Each model has its own strengths and weaknesses, which are summarized here. In general, the dynamic models perform as well as other state-of-the-art dynamical regional climate models, and the statistical model has comparable or superior skill, although for a very limited set of meteorological variables. As is typical of dynamical climate models, there remain uncertainties in simulating clouds, precipitation, and snow accumulation and depletion rates. Hence, the weakest aspects of the dynamical models are parameterized processes, while the weakest aspect of the statistical downscaling procedure is the limitation in predictive variables. However, the resulting simulations yield a better understanding of model spread and bias and will be used as part of the California probabilistic scenarios and impacts.

Keywords: California climate, baseline simulation, dynamic, and statistic downscaling, reanalysis

Executive Summary

Introduction

The California Energy Commission's Public Interest Energy Research (PIER) Program is developing regional climate change projections and scenarios for California that will be used for both state planning and research activities. Recent PIER reports have indicated a need to (1) further enhance the performance of regional climate models, and (2) inter-compare regional climate models, evaluating how well these models perform with such new enhancements when simulating California's climate. The Regional Climate Model Enhancement and Baseline Climate Intercomparison (REBI) study presented here has a goal of quantifying and comparing high-resolution regional climate model simulations of historical California climate to observations, each other, and to statistically downscaled simulations of climate. This project is required prior to the Regional Climate Model Analysis of Climate Change Sensitivities project.

Purpose

The purpose of this study is to perform a series of numerical simulations, both dynamic and statistically based, to determine regional climate model spread, and to generate a baseline set of model climatologies as part of the scenarios projection preparations. The follow-on climate projections project, Regional Climate Model Assessment of Climate Change Sensitivities, will use these results for better-understanding model biases, signal-to-noise, and to reduce model uncertainties.

Project Objectives

The objectives in the study were to enhance and develop California regional climate models and perform intercomparisons, as the first phase of the sensitivity analysis of projected climate change in California at fine scale. This analysis is of high value to the climate science research community, impact assessment community, and California policy makers.

Project Outcomes

The primary project outcome is a set of enhanced and intercompared regional climate models with an analysis of model spread, and diagnostic analysis for a subset of variables. The integration period, 1980–1989, has been examined for model performance and skill, and represents the baseline for impacts modeling and assessment. Variables that have been analyzed include: total precipitation, maximum and minimum daily surface air temperature, surface specific humidity, wind speed, snow water equivalent, and surface energy budgets.

Conclusions

The dynamically and statistically downscaled regional climate model results discussed in this report will be included in the development of probabilistic scenarios, and multiple variables in ensemble form will be applied to California impacts studies.

1.0 Introduction

California's climate, hydrology, and ecology represent one of the most diverse and sensitive regional systems in the United States, with over 1100 miles of coastline, desert regions, irrigated agricultural regions, and mountainous snowpack water storage regions. It has been determined in previous studies (Field et al. 1999; Hayhoe et al. 2004; IPCC 2001, 2007; USGCRP 2001; California Regional Assessment 2002; California Regional Scenarios 2006) that California's ecosystems, water resources, and infrastructure are at significant risk due to heat-absorbing atmospheric greenhouse gases (GHG) in the form of carbon dioxide, methane, nitrous oxide, and others from fossil fuels sources. In 2006 the California State Legislature passed, and the governor signed into law, Assembly Bill 32 (AB 32), the California Global Warming Solutions Act of 2006.[1] AB 32 establishes a "*first-in-the-world comprehensive program of regulatory and market mechanisms to achieve real, cost-effective reductions of greenhouse gases.*" (CARB 2008). It makes the California Air Resources Board (CARB) responsible for monitoring and reducing GHG emission reduction targets in California to 1990 levels by 2020. An Executive Order signed by the governor on June 1, 2005, mandates the California Environmental Protection Agency (CalEPA), in collaboration with other state agencies, to prepare biennial science reports on the potential impacts of climate change in California. CalEPA has requested the California Energy Commission's Public Interest Energy Research (PIER) Program to lead the preparation of these reports because PIER has had a strong climate change research sub-program since 2001. The biennial reports include impact studies to water supply, public health, energy, agriculture, the coastline, and forestry.

As an initial step towards fully quantifying the range of climate variability and change in California at high spatial resolution (10 kilometers, km), one statistical and four dynamical downscaling approaches are intercompared and evaluated against observations. The rationale here is to test the usefulness and appropriateness of the different climate downscaling techniques based on observational data availability, computational constraints, climate stationarity assumptions, and model parameterizations. Each approach has uniquely different, and in some cases similar, advantages and disadvantages.

Climate model evaluation and intercomparison provides quantitative evaluations of model and process performance using observations and other models as standards for comparison. It allows for model advancements, leading to reduced errors and improved model performance. Climate model intercomparisons are essential for understanding how model-simulated projections of the future compare with the present. Improved model performance will facilitate better decision making of the actions needed for climate change mitigation, adaptation, and coping strategies.

Since 1989, the U.S. Department of Energy's (DOE's) Program for Climate Model Diagnostics and Intercomparison (PCMDI) has led the intercomparison of global-scale general circulation models (GCMs). The PCMDI mission is to develop and apply improved methods and tools for the diagnosis and intercomparison of GCMs, and this effort represents a quality control

[1] Assembly Bill 32 (Nuñez), Chapter 488, Statutes of 2006

gatekeeper for the GCMs that are part of the Intergovernmental Panel on Climate Change (IPCC). While GCMs provide an important understanding of the climate on subcontinental and larger scales, they are unable to resolve fine-scale climate features and forcings that are of importance at local-to-regional scales; hence, downscaling techniques have and will continue to be an essential element of climate change impacts analysis.

Two main approaches are used to downscale global climate data: dynamical downscaling and statistical downscaling.

Dynamical downscaling uses a fine-resolution climate model having a global or smaller domain to produce fine-scale information. Physical knowledge comes from laws describing the atmosphere included in the fine-resolution model. If it has a limited geographical domain, this model is driven by initial and boundary conditions from a coarse simulation with a larger (typically global) domain. Required boundary condition data for limited-domain models includes three-dimensional atmospheric fields at three-hour or six-hour intervals. This approach involves a large data volume, and few climate modeling centers save the simulated three- and six-hour spatial output fields. Thus, most coarse-resolution climate simulations are restricted in the scale in which the output can be downscaled using a nested, limited-domain model. This restriction on such large-scale boundary conditions has recently been studied in detail by Yoshimura and Kanamitsu (2008), who proposed a method to relax this restriction. Global high-resolution simulations can be performed using only monthly mean sea-surface temperatures and sea ice concentrations as boundary data; this is available from virtually all simulations. Thus this technique is widely applicable; and it provides global downscaled data. It is, however, much more computationally demanding than using a limited-domain model. Dynamical downscaling in general is computationally demanding, but produces a complete range of physically consistent meteorological output. Because of this physical consistency, the output is useful for research on physical mechanisms of the local scale climate change. The most important shortcoming of dynamical downscaling is errors in the dynamical models (both nested and large-scale). Many of the model errors are systematic, but can be removed by using the differences or anomalies. This approach is frequently used in the study of changes due to global warming.

Statistical downscaling uses empirical, data-driven techniques to produce fine-scale climate information (Wilby and Wigley 2000). In the *constructed analogues* approach (Zorita and Storch 1999), relationships between local- or regional-scale climate features and large-scale features are developed by analyzing observations. Key assumptions in this approach are that the future climate patterns can be derived from linear combinations of the weather from a library of previously observed patterns, and that climate changes predicted using coarse-resolution models are correct at fine spatial scales. In another method, the *delta change or perturbation* approach, changes in key climate quantities (such as predicted temperature increases) from a coarse simulation are added (e.g., for temperature) or multiplied (e.g., for precipitation) to fine-scale historical climate data, producing a fine-scale future temperature or precipitation prediction. An advantage is that using predicted *changes* from climate models results in a first-order elimination of biases from these models. Some analogue approaches also include bias correction (e.g., Imbert and Benestad 2005). Statistical downscaling is computationally

inexpensive, but in general produces results for only a few meteorological quantities (e.g., precipitation and near-surface temperatures). Another disadvantage of statistical downscaling is the difficulty of uncovering physical mechanisms behind unexpected results.

An important difference between dynamical and statistical approaches is that the latter, being empirical, does not require knowledge or accurate characterization of specific climate forcings; poor knowledge of these forcings (e.g., aerosols and land-use effects) can limit the fidelity of dynamically based simulations. This can be a disadvantage, however, if forcings change significantly between the period used for the development and calibration of the statistical model and the period being simulated; hence significantly large changes in forcings may violate the stationarity assumption fundamental to statistical approaches.

In 2003, the California Energy Commission (Energy Commission) sponsored a series of road-mapping exercises, including the report, *Modeling Regional Climate Change in California* (Gates 2003). This report recommended the design of a regional climate model intercomparison protocol, control climate simulations, an evaluation and analysis of downscaling methods, development of a California database, and the development of a database access system. The present study builds upon the report recommendations, two previous California investigations to intercompare climate model physics and dynamics (Duffy et al. 2006; Kueppers et al. 2008), and several past and ongoing regional climate investigations, such as the Program to Intercompare Regional Climate Simulations (PIRCS, Gutowski et al. 1988, 1998, 2000; Takle et al. 1999), the North American Regional Climate Change Assessment Project (NARCCAP: Mearns et al. 2004), an Asian domain intercomparison (Leung et al. 1999; Fu et al. 2005), an Arctic regional climate model (RCM) intercomparison (Curry and Lynch 2002), and a European intercomparison (PRUDENCE: Christensen et al. 2007; Déqué et al. 2007; Jacob et al. 2007).

The next section provides details of the approach for intercomparing and evaluating downscaled California regional climate and model limitations. This is followed by an analysis of the results, significance, and applicability of each model with regard to impact and adaptation studies, and lastly a discussion with concluding summary.

2.0 Approach

The downscaling evaluation here includes one statistical and four dynamic approaches. To best evaluate the multi-model performance, domains, grids, and forcings were specified to be the same or as similar as possible. Each RCM used similar double-nested domains and resolutions (Figure 1) with the same set of lateral boundary conditions and input forcings, to generate 10-year baseline simulations for January 1, 1980, to December 31, 1989, at 30 kilometer (km) (outer nest) and 10 km (inner nest) resolutions. The lateral boundary conditions were evaluated to ensure the transition in length scale between the GCM (200 km) and the 30 km simulation did not impose jump discontinuities. An exception is the Regional Spectral Model (RSM), which downscaled directly from 200 km resolution global reanalysis to 10 km resolution.

Each model output includes a common set of variables and fluxes, mapped onto identical grids for analysis. This procedure follows the PCMDI protocols used for the IPCC Fourth Assessment Report (AR4) intercomparisons. The statistical methods used the same inner domain as shown

in Figure 1, but produced only precipitation and temperature fields at daily to monthly time-steps. In Subsection 2.1 dynamic and statistical methods used in this study are discussed; a discussion of input data follows in Subsection 2.2.

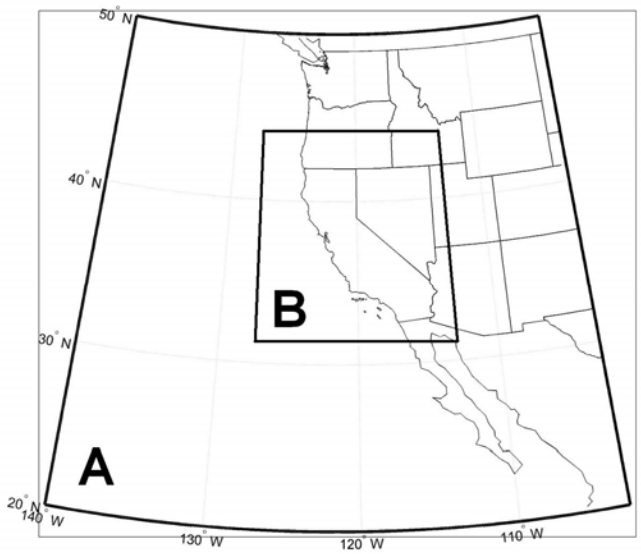

Figure 1. Model domains used in this study. A. Western United States and Eastern Pacific Ocean, 30 km resolution, [139W21N x 104W51N], B. California, Nevada, Eastern Pacific Ocean, 10 km resolution, [128W31N x 113W44N]

2.1. Dynamic and Statistical Downscaling

The Weather, Research, and Forecasting (WRF) model was developed at the National Center for Atmospheric Research (NCAR) by Skamarock et al. (2005). It has been enhanced by Lawrence Berkeley National Laboratory (LBNL) researchers to include the NCAR Community Land Model version 3 (CLM3: Oleson et al. 2004), an advanced land surface scheme with sub-grid representation, advanced snow processes, dynamic vegetation with plant functional types, and lateral hydrologic flow capability (Jin et al. 2007). In the version used in these studies, plant functional types are turned off and lateral hydrologic flow is a topographic distribution index representation for soil moisture redistribution per grid cell. We are not using any streamflow routing in this version. The enhanced code, WRF-CLM3, is set up with the Grell and Devenyl convection parameterization for cumulus clouds (Grell and Devenyl 2002), the Yonsei University planetary boundary layer (PBL) scheme (Hong and Pan 1996), and the Medium Range Forecast Model scheme (Mellor and Yamada 1982). The microphysics scheme used here is the WRF Single-Moment 3-class (WSM3) scheme (Hong et al. 2004). The Rapid Radiative Transfer Model (RRTM) is based on Mlawer et al. (1997) and is used for describing longwave radiation transfer within the atmosphere and to the surface; the shortwave radiation scheme was developed by Dudhia (1989) and further advanced by Chou and Suarez (1999).

The Regional Spectral Model (RSM: Juang and Kanamitsu 1994) originates from the regional spectral code originally developed at the National Centers for Environmental Prediction (NCEP). The code was updated with greater flexibility and much higher efficiency (Kanamitsu

et al. 2005) at the Scripps Institution of Oceanography (SIO). The RSM utilizes a spectral method (with sine and cosine series) in two dimensions. A unique aspect of the model is that the spectral decomposition is applied to the difference between the full field and the time-evolving background global analysis field. The model configuration and the downscaling methods are basically the same as that of CaRD10 (10 km California Reanalysis Downscaling; Kanamitsu and Kanamaru 2007), where the scale-selective bias correction (SSBC, Kanamaru and Kanamitsu 2007) was applied with a nudging scheme to the Reanalysis large-scale thermodynamic fields for a 10 km resolution simulation. Major updates from the CaRD10 project are: inclusion of the Noah land surface model (Ek et al. 2003) with four soil layers instead of the two-layered Oregon State University land surface model (Pan and Mahrt 1987); incorporation of cloud water and cloudiness as prognostic variables (Tiedtke 1993; Iacobellis and Sommerville 2000) for better precipitation prediction; a larger domain size: 19.506°– 50.193°N, 135.314°–103.587°W, which is 180% and 175% larger in zonal and meridional directions than those of the CaRD10, to improve summer time monsoon flow from the Gulf of California; narrower lateral boundary nudging zones, based on the Davies scheme (1983) and extends only 2.5% of the total width in each of four lateral boundaries instead of 11.5% in CaRD10 to increase the useable domain. Similar to WRF-CLM3, RSM does not include a routing scheme.

The International Center for Theoretical Physics (ICTP) Regional Climate Model, RegCM3 (Pal et al. 2007), is a third-generation regional-scale climate model derived from the National Center for Atmospheric Research-Pennsylvania State University (NCAR-PSU) MM5 mesoscale model. RegCM3 uses the same dynamical core as MM5. RegCM3 also includes the Biosphere-Atmosphere Transfer Scheme (BATS1E: Dickinson et al. 1993) for surface process representation and the CCM3 radiative transfer package (Kiehl et al. 1996). RegCM3 documentation and source code are available at the ICTP, Trieste, Italy site.[2] In this experiment, RegCM3 was configured with the Grell cumulus scheme (Grell 1993) utilizing the Fritsch and Chappell closure scheme (Fritsch and Chappell 1980) and the Holtslag boundary layer scheme (Holtslag and Boville 1993). This version of Biosphere-Atmosphere Transfer Scheme (BATS) has 22 land-cover types and 3 soil layers, with rooting depth and other soil properties linked to land cover type. Similar to the other models used here, it does not include a routing scheme. Table 1 provides a summary of the dynamic downscaled model settings.

[2] www.ictp.trieste.it/RegCNET/model.html.

Table 1. Summary of RCM settings

	RegCM3	RSM	WRF-CLM3	WRF-RUC
Land Surface	BATS1E Dickinson 1993	NOAH Ek et al. 2003	CLM3 Oleson et al. 2004	RUC
Soil Moisture Modification for Irrigation to "activate"	75% Field Capacity during the growing season	Saturation at all time steps	None	None
Microphysics	Orville and Kopp 1977	Iacobellis and Somerville 2003	Lin et al. 1983	WSM 3-class simple ice scheme (Hong et al. 2004)
Shortwave Radiation	Kiehl et al. 1996	Chou and Lee 1996	Chou and Suarez 1999	Chou and Suarez 1999
Longwave Radiation	Kiehl et al. 1996	Chou and Suarez 1994	RRTM Mlawer et al. 1997	RRTM Mlawer et al. 1997
Planetary Boundary	Holstag and Boville 1993	Hong and Pan 1996	Mellor-Yamada 1982	Mellor-Yamada 1982
Cumulus	Grell 1993	Moorthi and Suarez 1992	Grell and Devenyl 2002	Kain-Fritsch scheme Kain 2004

An earlier analysis of the role of irrigation settings on these RCMs was reported (Kueppers et al. 2008, Snyder et al. 2006) and will be referred to here in the discussion section.

The Constructed Analogues (CANA) statistical downscaling approach is based on the methods developed by van den Dool (2003) and has been presented by Hidalgo et al. (2008). The CANA method is based on the matching of daily Reanalysis weather patterns (e.g., precipitation and temperature) with 1/8 degree observational (12 km) weather patterns in an independent "library" of matching pairs of coarse-scale (Reanalysis) and corresponding high-resolution 1/8 degree (12 km) weather patterns (Maurer et al. 2002 data) for the same day. The 30 most similar historical patterns (analogues) to the Reanalysis pattern to be downscaled are used in a linear regression to produce a coarse-scale estimate for each day. The regression coefficients obtained from the coarse-scale analysis for each day are then applied to the corresponding 30 high-resolution analogue weather patterns to produce daily-downscaled estimates at 1/8 degree (Hidalgo et al. 2008). In this way, a large fraction of the daily variability of the weather patterns at high resolution is conserved. A comparison of the CANA method with the statistical method of bias correction following with spatial downscaling (Wood et al. 2004) can be found in Maurer and Hidalgo (2008). For the Regional Climate Model Enhancement and Baseline Climate Intercomparison (REBI) analysis the library of previously observed patterns was selected from the period 1950–1978 so the downscaling period (1979–1999) is independent of the library used to derive the analogues.

In Hidalgo et al. (2008), the linear predictor equations were trained and validated for the period 1950–1999, where the even-numbered years were used for model calibration and odd-number years were used for model cross-validation. The CANA method showed very good skill (day to day validation correlations of the downscaled estimates with the observed data on the order of 0.7 or more) in downscaling coarse-scale temperature to a 12 km grid, and in reproducing precipitation in the coastal states of the western United States, with less skill in the interior regions (Hidalgo et al. 2008).

2.2. Input Data

The National Centers for Environmental Prediction-Department of Energy Atmospheric Model Intercomparison Project II Reanalysis (NCEP/DOE-2) data were used for the dynamic model initial and lateral boundary conditions, as well as for training and validation of the CANA statistical model. The Sea Surface Temperatures (SSTs) were initialized with the Atmospheric Model Intercomparison Project (AMIP) dataset for WRF and RegCM, while the European Reanalysis 40-year SST data (ERA-40)3 was used for the RSM lower boundary conditions over the Pacific Ocean. This SST (Fiorino 2004) is a combination of the SST analyses from the Hadley Center, the United Kingdom Met Office (monthly mean HadISST, prior to and including 1981) and NCEP (weekly NCEP 2DVAR SST, after 1982 inclusive). It was cleaned up at the ice edges and interpolated to daily analysis using the mean conserving interpolation scheme (Taylor et al. 2000).

Model results are evaluated with the Parameter-elevation Regressions on Independent Slopes Model (PRISM) climatologies for California temperature and precipitation with monthly, yearly, and event-based climatic parameters (Daly et al. 2001, 2008). PRISM is a unique knowledge-based system. It includes point observations, digital grid estimates, digital elevation maps, and expert knowledge of climatic extremes, including rain shadows, coastal effects, and temperature inversions. It uses climate mapping technology and climate statistics to provide a continuous, quantitative confidence probability for each observation, estimate a replacement value, and confidence intervals. The PRISM data has been subjected to categorical quality checks to ensure there is observational validity (Daly et al. 2004). While not exact, the resulting PRISM climatologies are often taken as *near-truth* data sets and are used for numerous applications, including impacts analysis. Other simulated quantities are evaluated against the North American Regional Reanalysis (NARR)[4] dataset. NARR is a fine-resolution reanalysis data product based on the Eta limited-domain model. Noteworthy features of NARR include direct assimilation of precipitation and some radiative fluxes. We use NARR to compare simulated quantities such as radiative fluxes for which adequate observations are not available. Figure 2 indicates that PRISM minus NARR results in (A) PRISM (NARR) precipitation being overestimated (underestimated) along the mountain regions, (B) PRISM (NARR) slightly cool (warm) in the Central Valley for DJF Tmax, (C) PRISM and NARR JJA Tmax very close, except a few grid cells, and (D) PRISM is generally cooler than NARR for JJA Tmin.

[3] www.ecmwf.int/research/era/do/get/era-40.

[4] www.emc.ncep.noaa.gov/mmb/rreanl/.

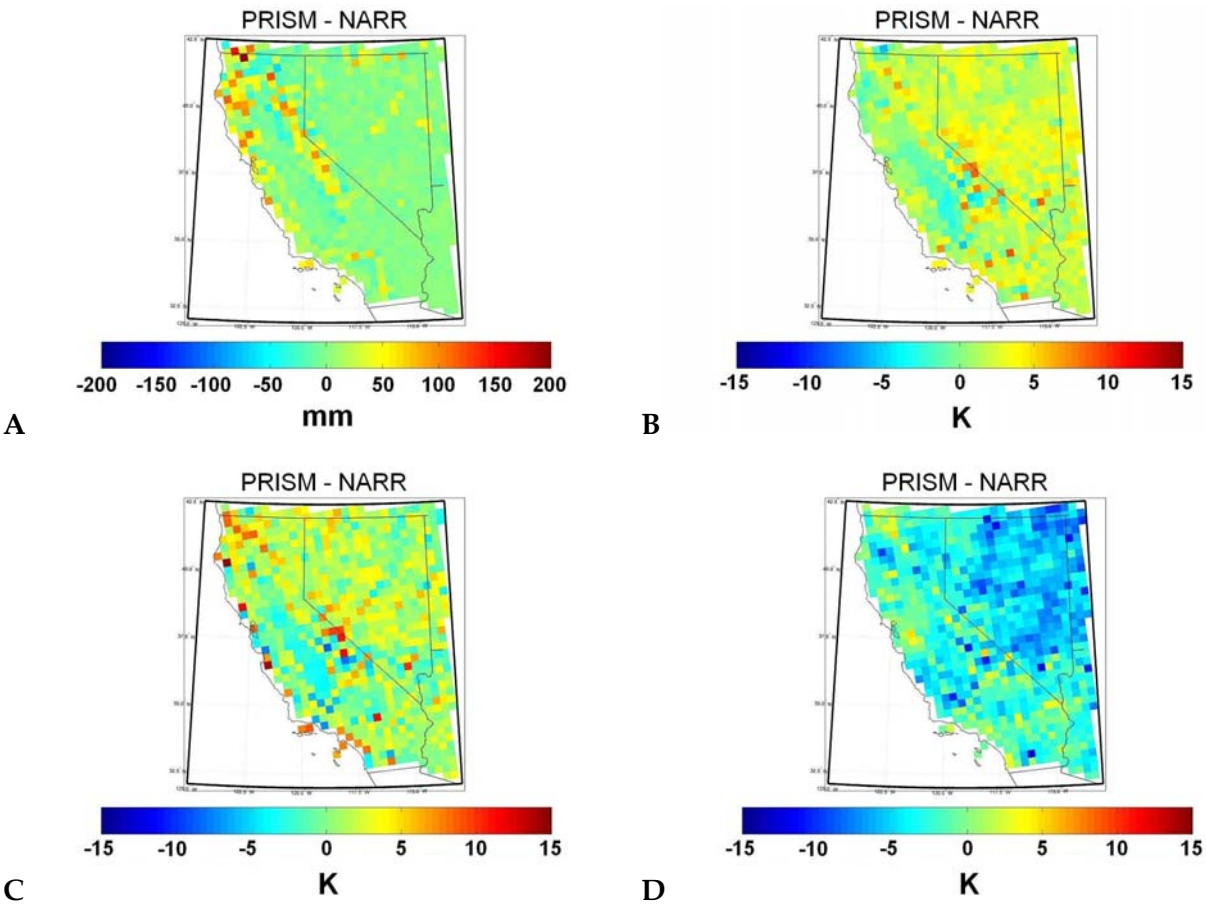

Figure 2. Climatological (1980–1989) differences between the PRISM and NARR for (A) NDJFM precipitation, (B) DJF Tmax, (C) JJA Tmax, and (D) JJA Tmin

Results of all REBI project simulations were converted to a common format that adheres to standards developed for the climate and weather forecast (CF) community. The *CF conventions* specify standard variable names, dimension names, coordinate systems, calendars, metadata, etc.[5] REBI model outputs were interpolated in the vertical to a standard set of atmospheric pressure levels. For certain analyses, such as calculating inter-model differences, results were interpolated to a common latitude/longitude grid having approximately the same 10 km grid spacing as the original RCM coordinate grids (1/12 degree in latitude and longitude).

3.0 Results

Model results, bias, and uncertainty are presented and discussed, however due to the time and resource constraints of this project, uncertainty reduction is not reported here, only model spread. In the following subsections we provide a discussion on model differences with

[5] http://cf-pcmdi.llnl.gov/documents/cf-conventions/1.0/cf-conventions.html.

preliminary analyses of the mechanisms causing these differences. Detailed process-level analysis is not comprehensive in this report, it is ongoing, and is not the main objective here.

3.1. Climatological Means of Temperature and Precipitation

Three dynamic downscaling models (RegCM3, RSM, WRF-CLM3), one statistical downscaling method (CANA), and a commonly used, off-the-shelf, version of WRF (Weather, Research, and Forecasting-Rapid Update Cycle [WRF-RUC]), are evaluated and intercompared for model skill, as forced with the NCAR/NCEP Reanalysis II fields for 1980–1989. The climatological 10-year mean maximum and minimum 2 meter (m) air temperature and cumulative precipitation are shown for the winter and summer periods in Figures 3–5.

Figures 3a and b show spatial maps of California 10-year climatologies for June–August (JJA) daily maximum and minimum 2 m air temperature (T_{max}, T_{min}), respectively. The JJA maximum temperatures are well represented, with all models reproducing the large-scale spatial pattern of observed temperatures within the study domain. Nonetheless, all models have some local biases. CANA and WRF-CLM3 show small cold biases along coastal regions. RSM is too warm (by 3°C–5°C) throughout the Central Valley, South Coast, and Sierra Nevada regions. WRF-CLM3 has a strong cold bias in part of the Sierra Nevada, and is consistent with the existence of year-round snow (discussed below) in that region. RegCM3 shows overestimates near the coasts and in the south (i.e., 3°C–7°C) over a smaller area than WRF-CLM3, but is too cold in the Central Valley. This may be a partial result of the representations for irrigation (Table 1). Irrigation is difficult to include in models for CA since each farming region, each farmer, and each crop type has different irrigation requirements by season, and weather-year type. As noted below, this results in excessive latent heat fluxes, and hence a local cold bias. WRF-RUC shows larger JJA T_{max} overprediction for the Central Valley than WRF-CLM3. Similarly, the JJA minimum 2 m air temperature shows that the CANA performs well, with very slight underestimates along a north-south inland region, RSM overestimates T_{min} near the coast and southern inland regions, with some overestimates in the southern foothills and mountains, WRF-CLM3 appears to have topographic over- and under-estimates, with significant overestimates in the inland south similar to RSM. RegCM has topographic over- and under-estimates, but is somewhat less severe than WRF-CLM3. Comparison of results of WRF-RUC and WRF-CLM3 to those of the other models shows that the simulated near-surface temperatures are roughly as sensitive to the land-surface scheme as other aspects of the model.

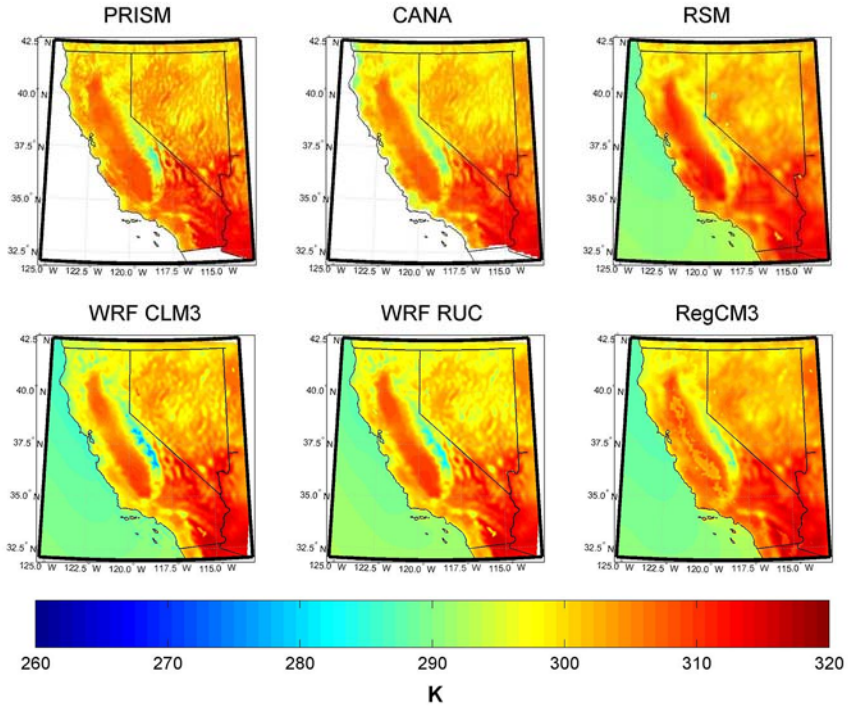

Figure 3a. Seasonal mean of daily maximum 2 m air temperature during June–August. Results shown are climatological means for 1980–1989.

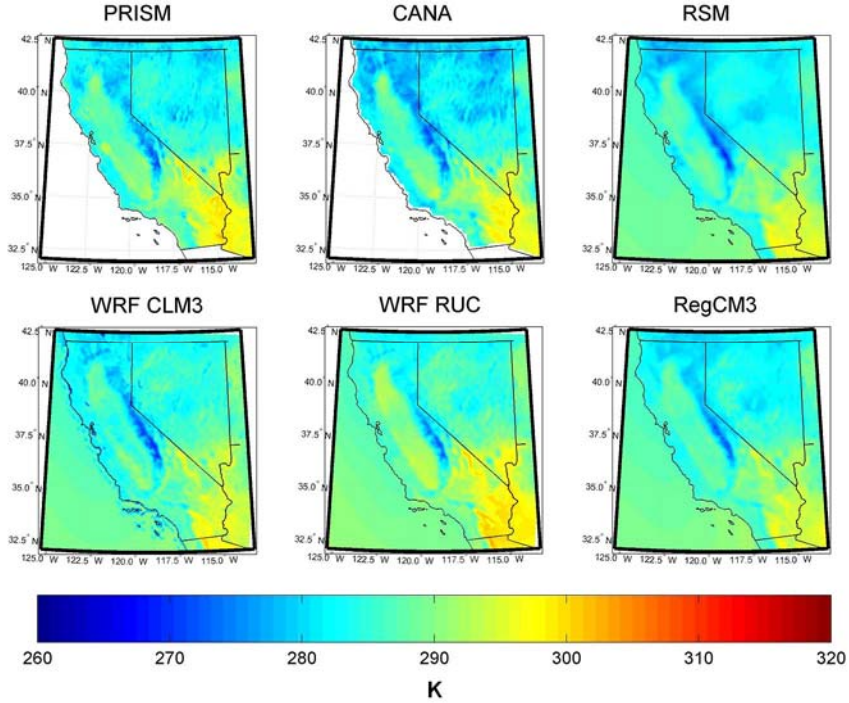

Figure 3b. Like Figure 3a, except for JJA daily minimum temperatures.

The winter December-February (DJF) maximum and minimum 2 m air temperatures (Figures 4 a and b) behave quite similar to the JJA temperatures, revealing slight overestimates for T_{max} in all cases, especially WRF-RUC and RSM in the Central Valley region. The DJF T_{min} differences (not shown) suggest that CANA tends to have negative biases, whereas all the dynamical models (especially WRF-RUC) are slightly too warm. The new coupling of CLM3 to WRF shows a dramatic reduction in this overestimate of T_{min}, but both WRF-CLM3 and RegCM are still too warm for DJF. These differences in near surface temperature likely involve differences in land surface treatments (CLM-3, Noah, and BATS) used in the three enhanced regional climate models. Full understanding of the temperature difference would require understanding the effects of differences in specified land characteristics (vegetation type, surface roughness, albedo, and soil type), as well as radiation fluxes and near-surface meteorological parameters.

The cumulative November to March (NDJFM) precipitation and difference, as compared with the PRISM NDJFM precipitation climatologies, are shown in Figures 5a and b, respectively. Considerable effort was put into the evaluation and enhancement of models to optimize convective schemes (Shimpo and Kanamitsu 2008; Jin et al. 2008), and to evaluate the SST sensitivity (Jin et al. 2008). All the models capture the large-scale spatial distribution of precipitation, which is dictated primarily by lateral boundary data and by topographic variations. However, the models exhibit significant biases in precipitation amounts: RegCM3, WRF-RUC, and to a lesser extent RSM are too wet in Sierra Nevada Mountains and in the wet Northwest part of the State. The difference plots in figure 5b show that CANA has smaller precipitation biases than any of the dynamical models, while WRF-CLM3 has the smallest biases among the dynamical models, and is mainly due to the cumulus scheme, and not irrigation, which has a small effect in comparison. The good skill shown in CANA would be expected, since the CANA approach relies on observation fields. WRF-RUC and RegCM3 are too wet everywhere in the State except the dry Southwest region. RegCM3 and RSM seem to have insufficient latent heat fluxes over the ocean (figure 10), particularly off the coast of Northern California. This makes the model's wet bias more remarkable, since not only is the incorrect amount of moisture entering the model domain, but also ocean evaporation is contributing too little to the water available for precipitation.

Overestimation of precipitation in an area of large precipitation amounts is a common problem in high-resolution regional models. A smaller bias in WRF-CLM3 resulted when we used the Kain and Fritsch parameterization scheme, instead of the Grell and Devenyl (2002) scheme. A similar reduction in bias was observed in RSM test runs using Kain and Fritsch, as well, but the high computer cost of this parameterization prevented its use in this study.

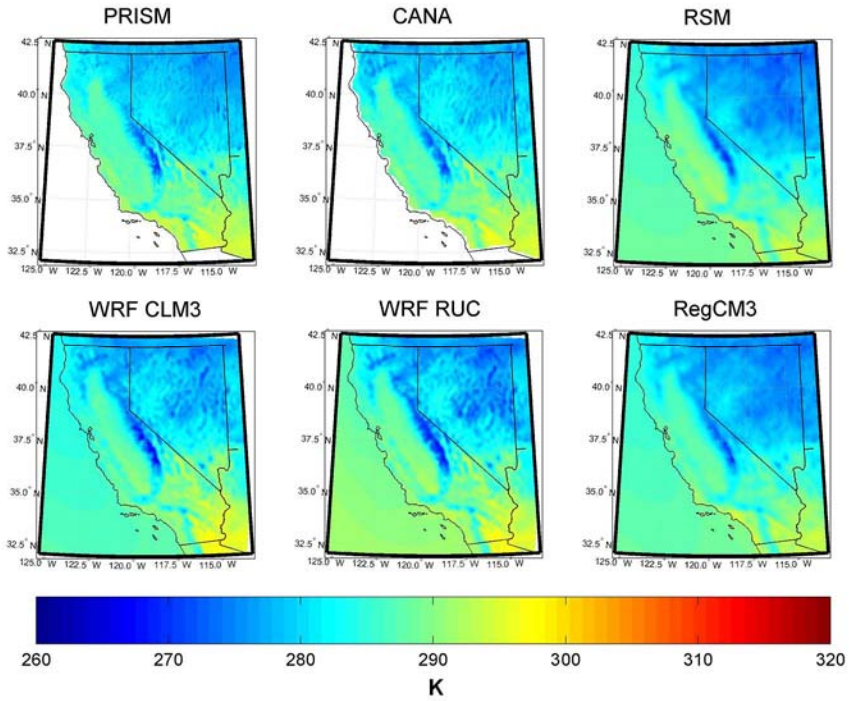

Figure 4a. Seasonal mean of daily maximum 2 m air temperature during December–February

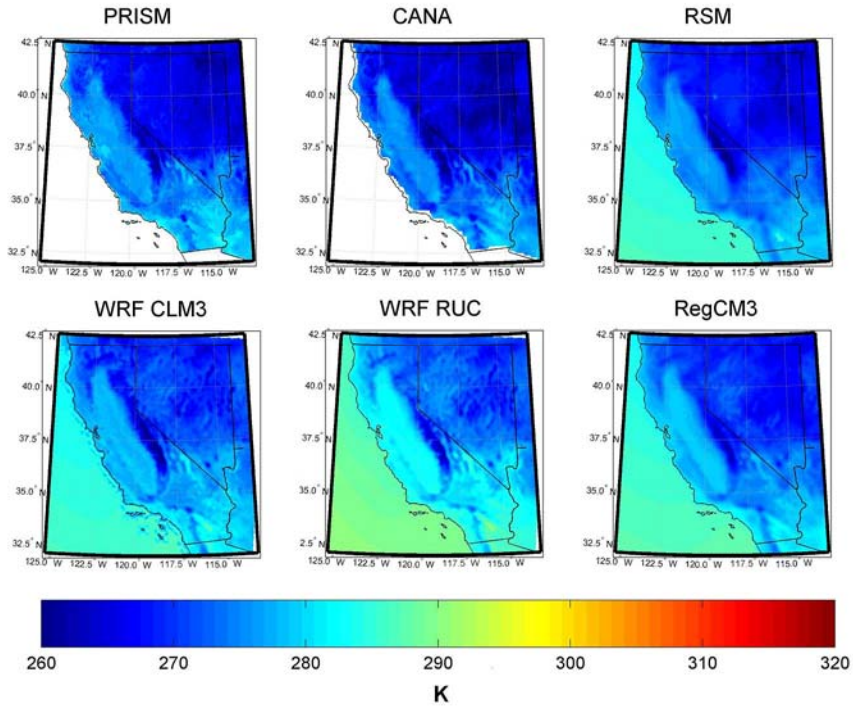

Figure 4b. Like Figure 4a, except for DJF daily minimum temperatures

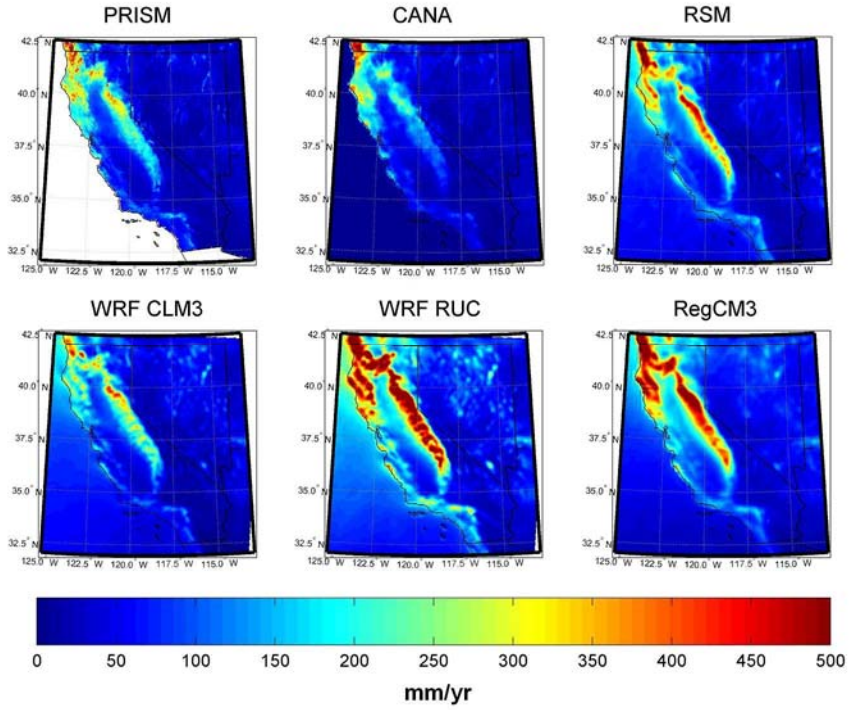

Figure 5a. Cumulative November–March precipitation, climatological mean for 1980–1989

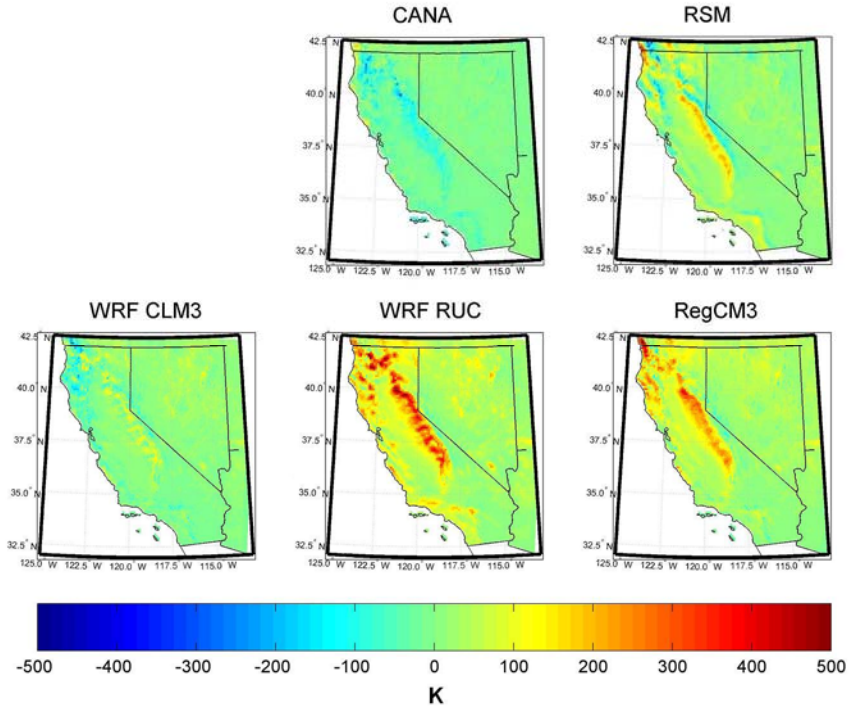

Figure 5b. Cumulative November–March precipitation differences relative to PRISM

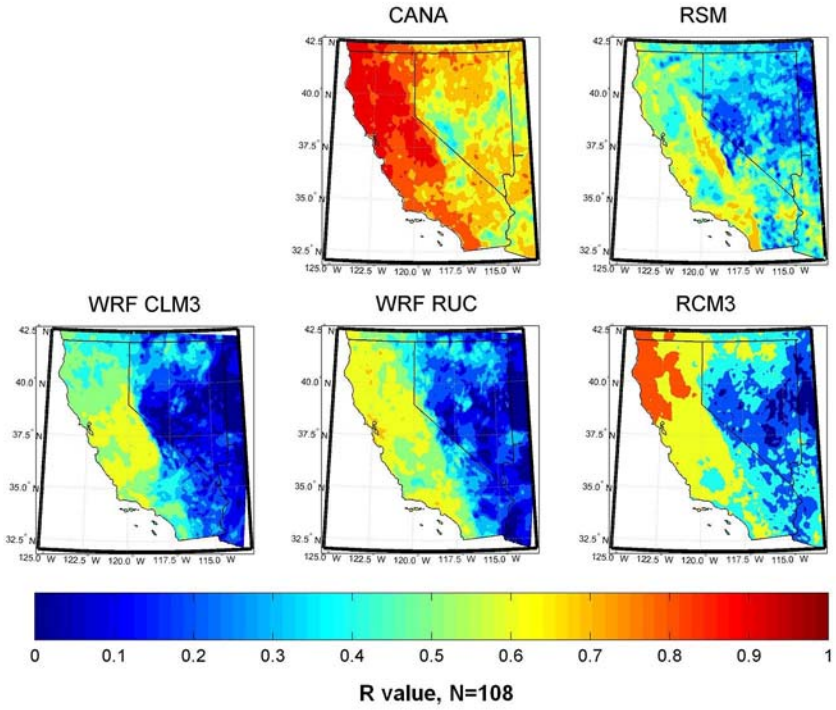

Figure 5c. Temporal correlations between monthly mean precipitation in models and the PRISM observation-based data set, based on the climatological mean for 1980–1989

Model-based cumulative monthly precipitation is correlated in time with the PRISM precipitation in Figure 5c. The statistically downscaled CANA precipitation has excellent correlation with PRISM, with most of the correlation space (R field) at or above 90%. The dynamic models cannot reach such high levels of correlation, however, RegCM3 does perform quite well (R > 90 percent) in the far northwest, while RSM is between 40% and 70% correlation, with its highest values showing up in the southern Sierra Nevada region. WRF-CLM3 has somewhat higher correlation values over a larger spatial domain, representing an improvement over WRF-RUC.

3.2. Snow Water Equivalent

Accurate simulation of snow is important for studies of water resources and other societal impacts. Snow is a particularly difficult quantity to simulate due to its sensitivity to both meteorology (temperature and precipitation) and land surface processes. Furthermore, even if the atmospheric and land surface model physics are correct, snow in California will tend to be under-simulated as a result of finite model resolution; this results in truncated elevations in the mountains, and hence overestimated surface temperatures.

Figure 6 indicates Snow Water Equivalent (SWE) for the 1980–1989 integration, using WRF-CLM3, WRF-RUC, RegCM3, and COOP observations[6] (NWS 2000; NRC 1998) over a Sierra Nevada sub-domain. (SWE results from RSM are discussed below, and CANA does not predict SWE). Alone among the models, WRF-CLM3 does a good job of simulating winter snow amounts, including year-to-year variability. As a result of this, its correlation coefficient against observed snow amounts (R=0.84) is higher than that of the other models. (R=0.61 for RegCM3 and R=0.50 for WRF-RUC). WRF-CLM3's cold bias in nighttime DJF temperatures in the Sierra probably does not affect simulated snow amounts, since even observed nighttime temperatures in this season and region are below freezing. It is striking that WRF-RUC and RegCM3 underestimate winter snow despite over-estimating winter precipitation. On the other hand, WRF-CLM3, and, to a lesser extent, RegCM3 erroneously preserves some snow cover throughout the year, even though RegCM3 significantly underestimates winter SWE.

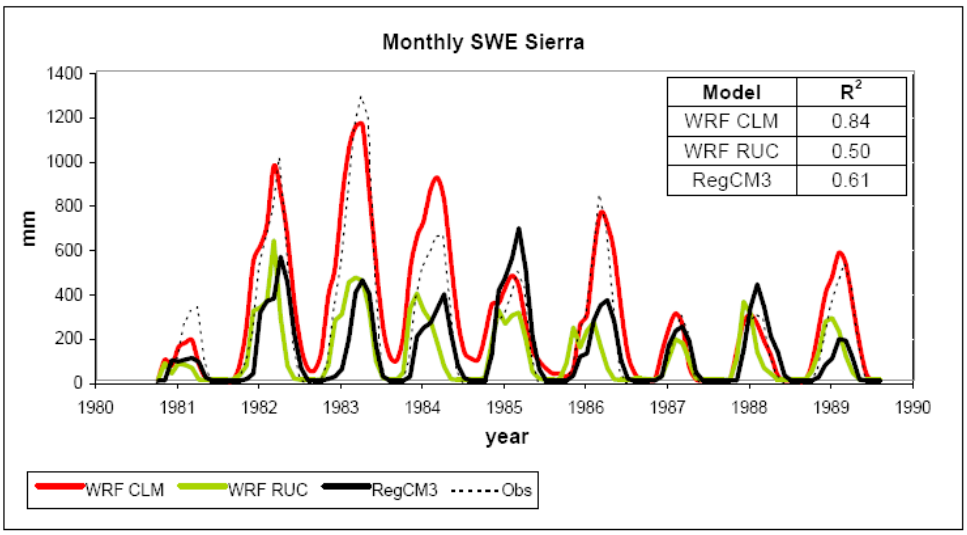

Figure 6. Top: Spatial mean Snow Water Equivalent (SWE) in a Sierra Nevada subdomain for WRF-CLM, WRF-RUC, and RegCM3 with COOP observations.

Other recent RCM evaluations (e.g., Leung and Qian 2003; Duffy et al. 2006) have attributed a significant fraction of errors in simulated SWE to deficiencies in land-surface models (as opposed to meteorology). Slater et al. (2001) demonstrated the sensitivity of simulated SWE to land surface treatments, by forcing 18 off-line land-surface models with observed meteorology. In our simulations, WRF-CLM3 has a strong cold bias in JJA daily maximum temperatures in the Sierra Nevada Mountains. Thus the erroneous persistence of snow in this simulation could be a consequence of meteorological biases (although the presence of snow will amplify a cold bias). On the other hand, RegCM3 does not have a spatially consistent bias in maximum JJA temperatures in the Sierra. Hence in this simulation the summertime snow is likely due to a land-surface problem.

[6] www.weather.gov/os/coop/coopmod.htm.

The RSM model simulated near-zero SWE at SNOTEL locations throughout the study period. One reason is that two SNOTEL stations are located on within grid cells in RSM that also include a large body of water (Lake Tahoe) and this may have affected the representation of RSM-simulated SWE. In addition, the RSM has a warm bias in near-surface temperatures on the lee side of the Sierra Nevada Mountains, and most of the precipitation there falls as rain, and precipitation is underestimated on the lee side. The SNOTEL stations for this sub-region are located near Lake Tahoe which happens to be the area where the ratio of snowfall-to-precipitation decreases to a very low value in RSM. Also, most of the SNOTEL stations are on the leeward of the Sierra (at least in RSM topography), so there is very little snowfall in RSM. The SWE over the windward side and higher elevation regions seem to be a little more reasonable in RSM. The model precipitation and snowfall is very sensitive to small changes in topography and elevation in this area and care should be taken when selecting representative locations for evaluation of simulated SWE.

3.3. Spatio-Temporal Variability

Looking beyond biases in seasonal mean quantities, Taylor diagrams (Taylor 2001) provide a convenient means to identify pattern correlations and RMS errors between simulated and observed quantities, as well as a simple evaluation of the spatiotemporal variability of simulated quantities. Figure 7 shows Taylor diagrams of near-surface air temperature, precipitation, and SWE in our simulations. These diagrams are based upon monthly mean quantities, mapped to a common spatial grid. The angular coordinate is the correlation coefficient between simulated and observed quantities, based on monthly mean results at each grid cell. This coordinate value evaluates if maxima and minima in the simulations occur at the correct times and geographic locations, but is independent of any errors in the magnitude of spatiotemporal variability. The latter is evaluated by the radial coordinate, which is the standard deviation of the results for each model for each month and grid cell, normalized by the same quantity in observations. (Again, this is calculated from monthly mean quantities at each grid cell, and thus reflects combined space and time variability.) The added value of a Taylor diagram is that the distance on the plot from the point marked "REF" on the horizontal axis is a normalized root mean square (RMS) error; thus the Taylor diagram displays three useful statistical measures on a two-dimensional plot. All these measures are independent of errors in the mean (i.e., biases), so the Taylor diagrams complement information presented so far.

The Taylor diagrams show that all the simulations do well at representing spatiotemporal variability in daily minimum and (especially) daily maximum near-surface air temperatures. The CANA results come close to matching the best of the dynamical models (RSM) in this respect. For precipitation, CANA again performs better than all the dynamical models except the RSM, despite seriously underestimating spatiotemporal variability. The excessive spatiotemporal variability of precipitation in RegCM3 and WRF-RUC seen in the Taylor diagram is due at least in part to these models' excessive precipitation in Northwest California and the Sierra Nevada mountains (Figure 6a). RegCM3 and WRF-RUC in particular underestimate the spatiotemporal standard deviation of SWE; this is consistent with these models having far too little SWE in winter.

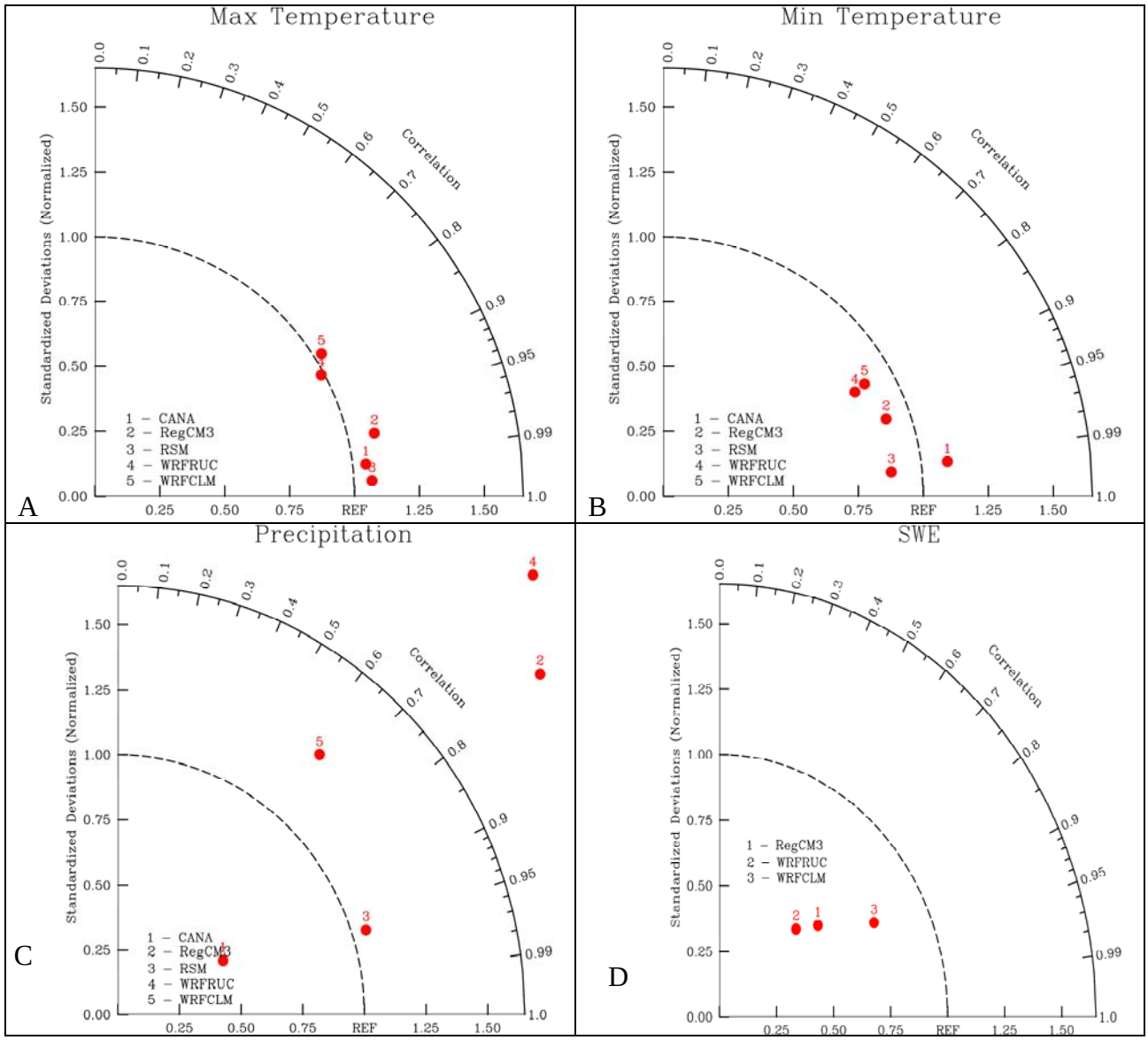

Figure 7. Taylor diagrams showing WRF-CLM3, WRF-RUC, RSM, and RegCM model-to-observation performance scores based on normalized standard deviations and correlations for monthly means of (a) maximum temperature, (b) minimum temperature, (c) precipitation, and (d) SWE

3.4. Surface Energy Fluxes

In general, apparent biases in simulated surface energy fluxes can reflect deficiencies either in the models being evaluated or in NARR, which we use as a standard for comparison. (Of course apparent biases can always result from errors in the observational standard, and we emphasize the possibility here since NARR is a model-based data product.). In some cases, as noted below, inter-model differences are at least as large as the differences between individual models and NARR. This implies significant biases in at least some of the models, regardless of any possible

errors in NARR. Furthermore, in some cases noted below, biases in simulated surface energy fluxes clearly result from deficiencies in other aspects of the simulation.

As with other aspects of simulated climate, biases in surface energy fluxes can reflect errors in imposed climate forcings, as distinct from a model's representation of physical processes. For example, RegCM3 shows (Fig. 8) much higher latent heat fluxes in the Central Valley in JJA than NARR (and the other models). This results from enhanced soil moisture in RegCM3, which is imposed as a way of representing the climatic effects of large-scale irrigation. Soil moisture content in RegCM3 was constrained to be 75% of field capacity in irrigated regions and seasons. This simple representation of irrigation also influences JJA sensible heat fluxes in RegCM3 to be lower (Fig.9b). More generally, biases in simulated seasonal-mean latent heat fluxes (Figure 8) appear to correlate with biases in the seasonal mean of daily maximum temperatures.

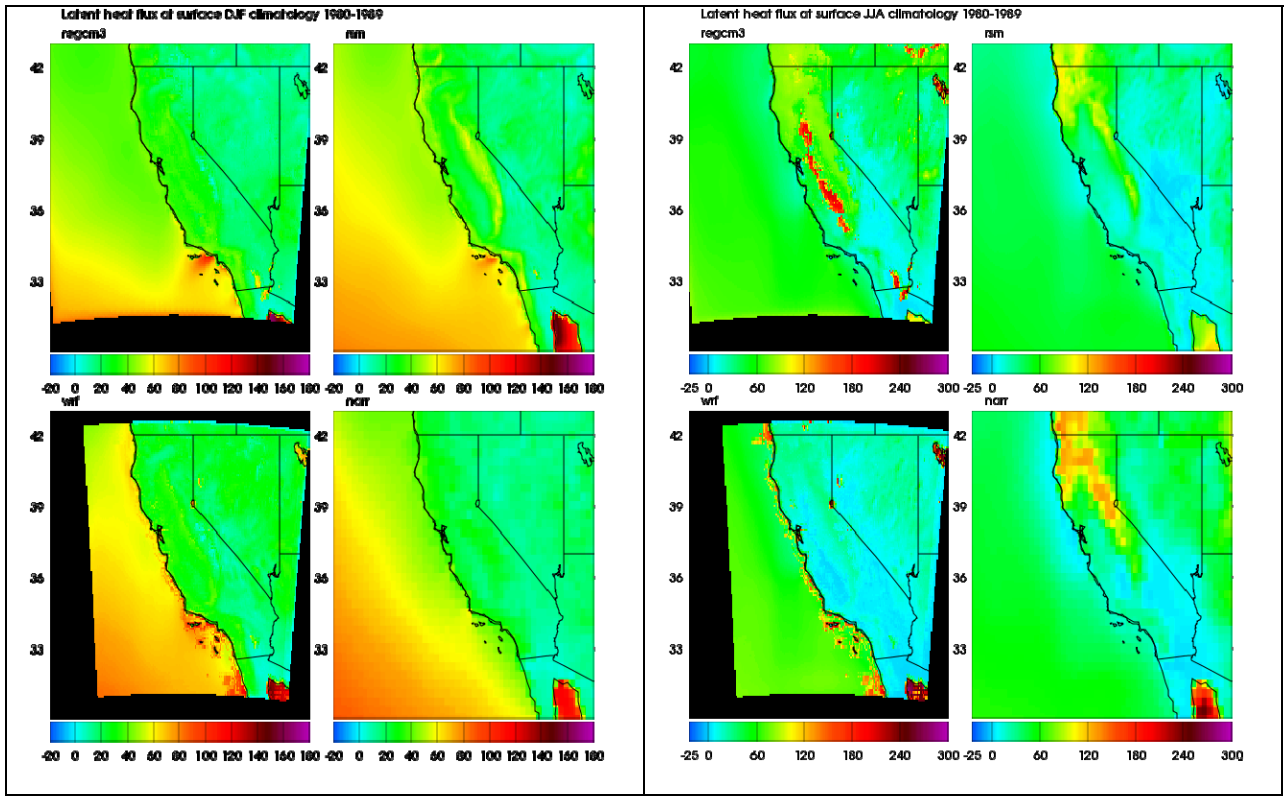

Figure 8. Regcm3, RSM, WRF-CLM, and the North American Regional Reanalysis (NARR) climatological (1980–1989) surface latent heat fluxes. for (A) DJF and (B) JJA

The increased latent heat flux just off the coast of Los Angeles during DJF is a reflection of an increase in Santa Ana events (Miller and Schlegel 2006; Kanamitsu and Kanamaru 2007); this is very clearly shown in RegCM3 and RSM (somewhat obscured in WRF), but is not found in NARR. This is due to the coarse resolution (32 km) used in NARR. The WRF simulation tends to have maximum evaporation just off the coast, which is very different from other models.

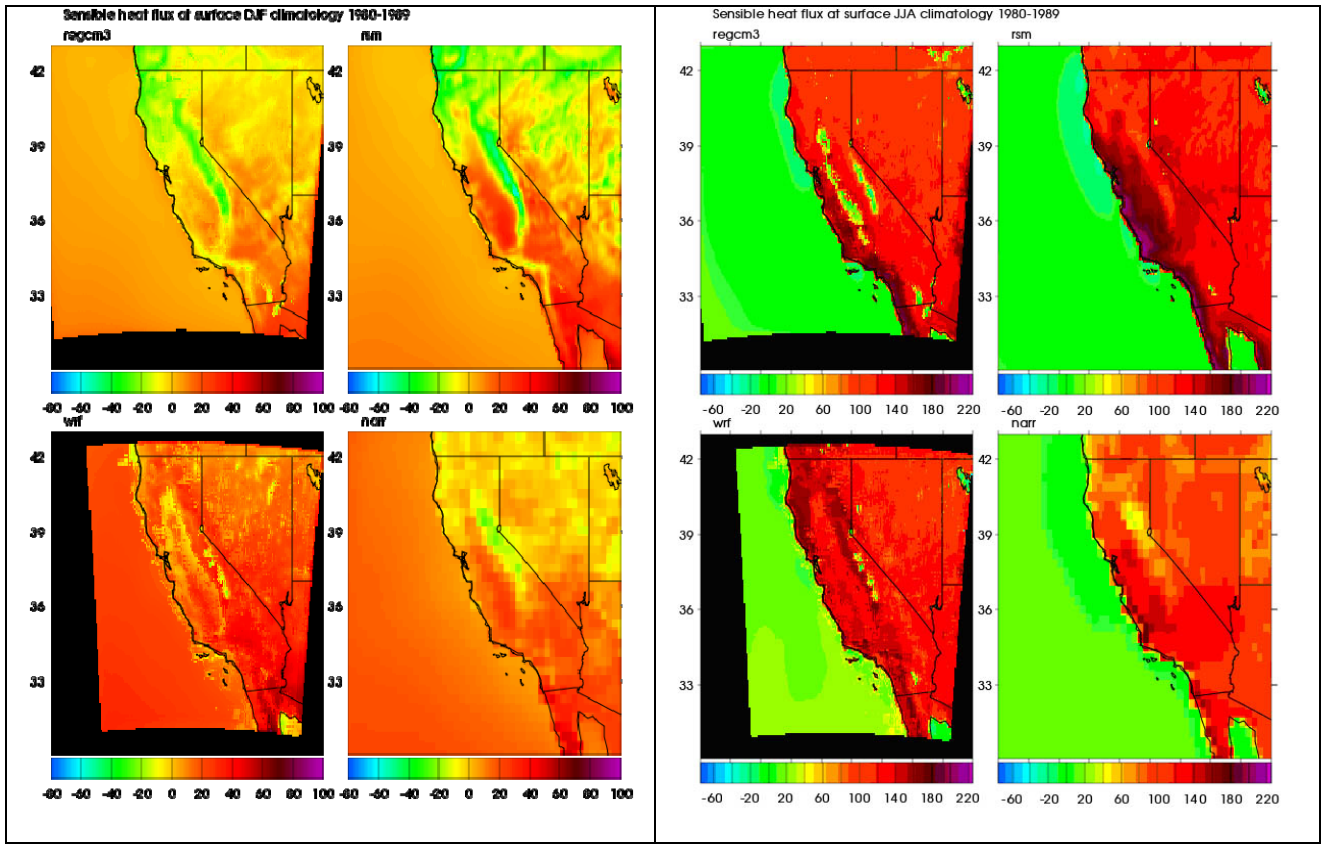

Figure 9. Regcm3, RSM, WRF-CLM, and the North American Regional Reanalysis (NARR) climatological (1980–1989) surface sensible heat fluxes for (A) DJF and (B) JJA

Downwelling longwave radiation (RLDS) at the surface (not shown) reflects atmospheric temperature and moisture distributions as well as cloudiness distributions. RLDS is fairly similar among the models. The larger RLDS over ocean in WRF is consistent with its small downwelling short wave flux and is presumably due to thick clouds. Again, RSM is very similar to NARR, but other models have clear positive biases, particularly over land.

NARR results for surface downwelling solar fluxes (not shown) exhibit the expected large-scale features: fluxes are higher in summer than winter, in winter are lower in the northern part of the State, and in summer are lower over the ocean. The biases in WRF-CLM3 and RSM in downwelling solar radiation are consistent with their biases in vertically integrated cloud fraction (Figure 10). The RSM model captures NARR's large-scale pattern of downwelling solar fluxes well in both seasons. All the models have relatively small biases in downwelling solar fluxes over land in summer, indicating that they are doing an adequate job of simulating the relatively little cloud cover in that season and region. Over ocean, however, WRF has too little downwelling solar, and RegCM3 has too much. The largest cloud bias in RegCM3 is over Nevada, but the model's precipitation bias in largest in California. This presumably indicates reduced available moisture after air masses have passed over the California mountains. Over-land biases in downwelling solar are larger in winter; this is expected, since cloud cover, and hence potential for biases in cloud cover, are greater in winter. WRF-CLM3's spatial pattern of

downwelling solar flux is very different from that of the other models in both DJF and JJA. This presumably results from cloud biases, but this cannot be verified due to lack of availability of cloud results from WRF-CLM3.

The largest local biases and apparent biases in upwelling solar fluxes (Figure 10) have to do with deficiencies in simulated snow cover. In DJF, all three models have much stronger solar radiation upwelling from the surface in the mountain regions than NARR does; this is largely a result of insufficient snow cover in NARR, due to its relatively coarse grid spacing (32 km). Hence this apparent model bias primarily reflects a limitation of NARR. On the other hand, both WRF-CLM3 and RegCM3 have a strong local maximum in upwelling solar in the mountains in summer (JJA). This is a consequence of these models having year-round snow in this region (discussed above), which is not observed.

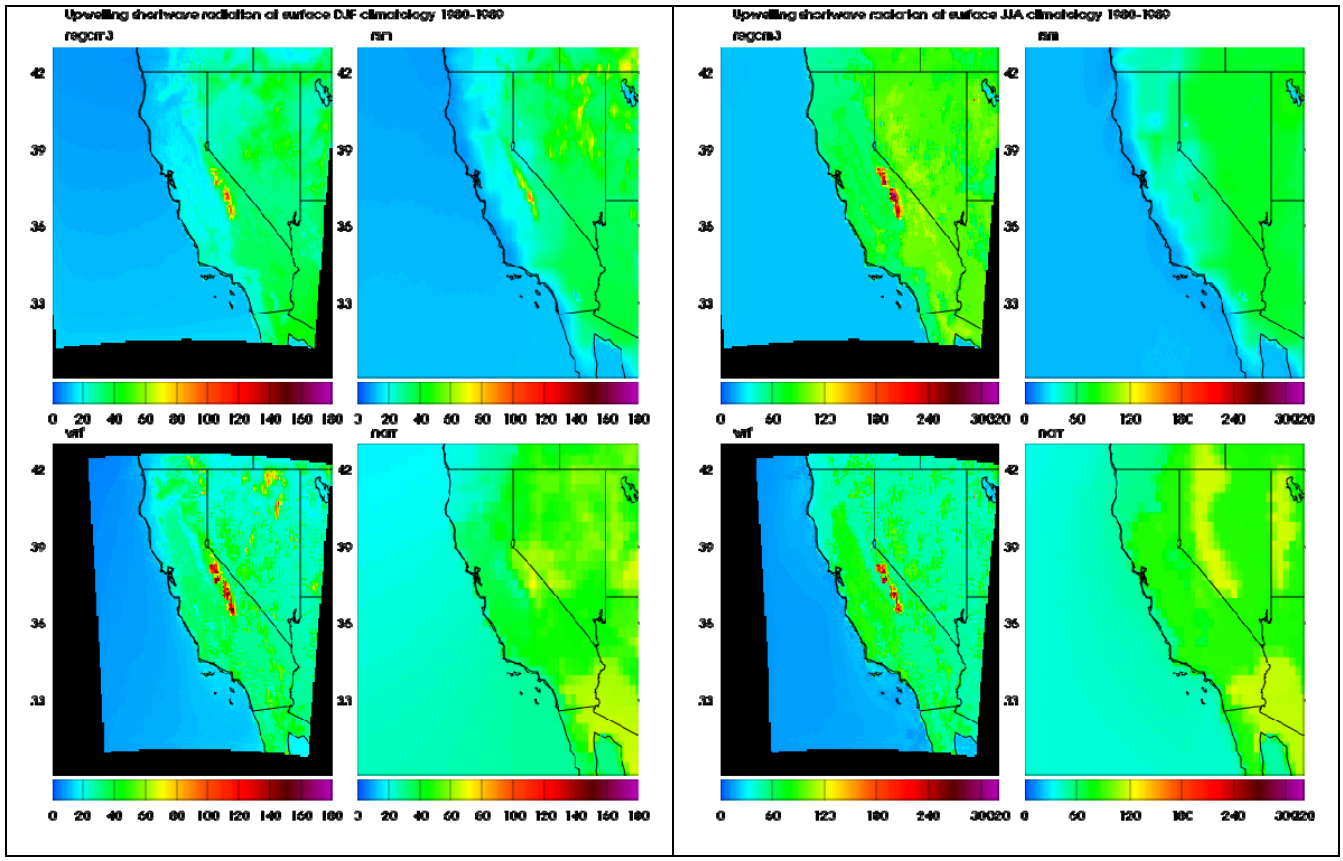

Figure 10. Same as Figure 9, except showing upwelling solar radiation at the surface

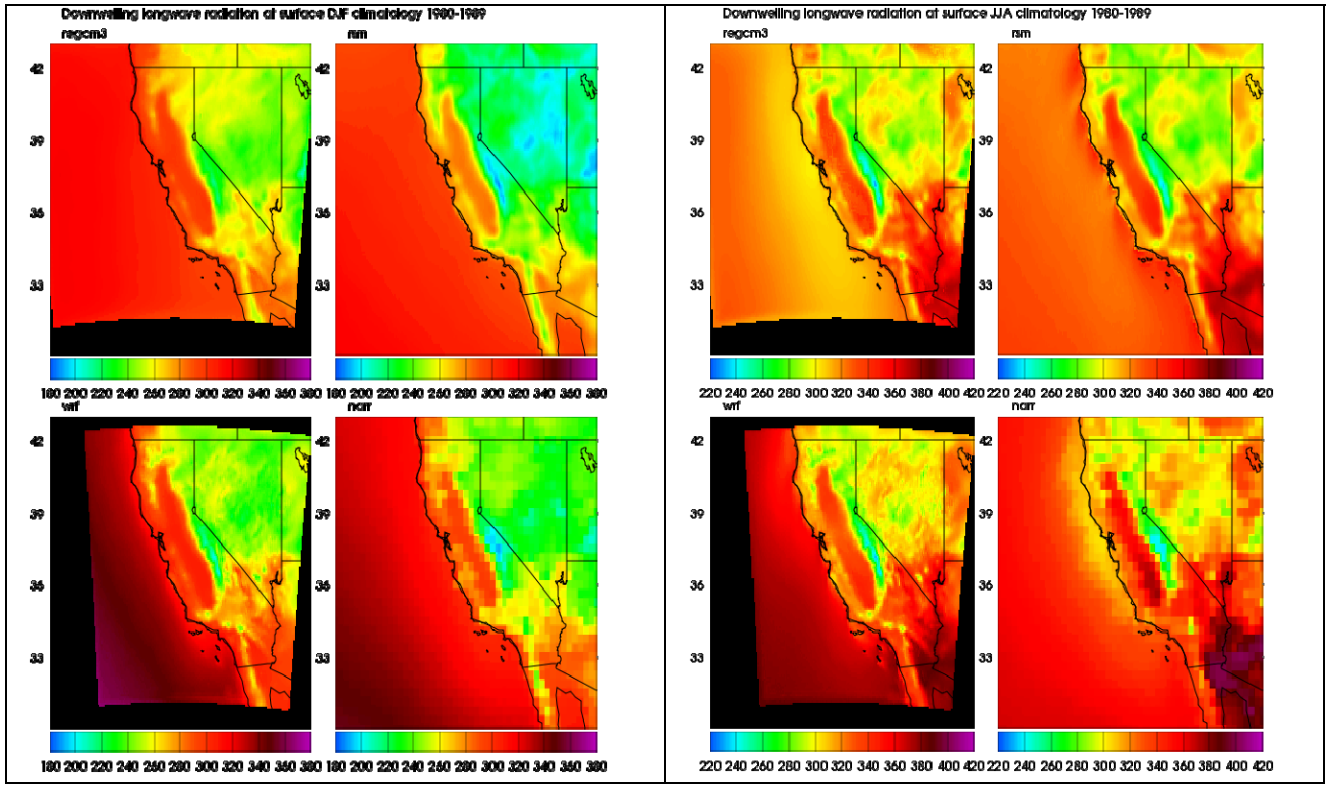

Figure 11. Same as Figure 10, except showing *downwelling longwave* radiation at the surface

3.5. Geopotential Heights and Surface Winds

The January 10-year climatological mean-monthly spatial plots of 500 millibar (mb) geopotential height is shown in Figure 12a. The January height fields show that all the models tend to be a little too high, when compared with reanalysis data. For July, the spectral RSM replicates the large-scale reanalysis forcing, while the RegCM3 underestimates height fields and the WRF appears to capture more detail associated with topographic disturbances (Fig. 12b). This is further seen in Figure 13, where simulated mean-monthly geopotential heights are plotted against the NCEP/NCAR Reanalysis heights for three points: P1 (120W, 39N, American River Basin), P2 (117.5W, 37N, Merced Basin), and P3 (122.5W, 38N, Russian River Basin). A general conclusion that can be drawn from these results is that WRF underestimates geopotential heights, especially when the reanalysis heights are low.

Model-simulated and NARR reanalysis surface wind speed and direction are plotted for mean-October 1982 (Figure 14a) and mean-January 1983 (Figure 14b). During this strong El Nino year, October coastal wind tend to flow northward following the land-sea interface. Each model does a fairly good job in capturing this detail, with RegCM showing stronger inland local circulation patterns. During the winter, when storminess is at a peak, the models diverge with WRF showing a strong onshore flow in Northern California, and RegCM exhibiting a strong offshore

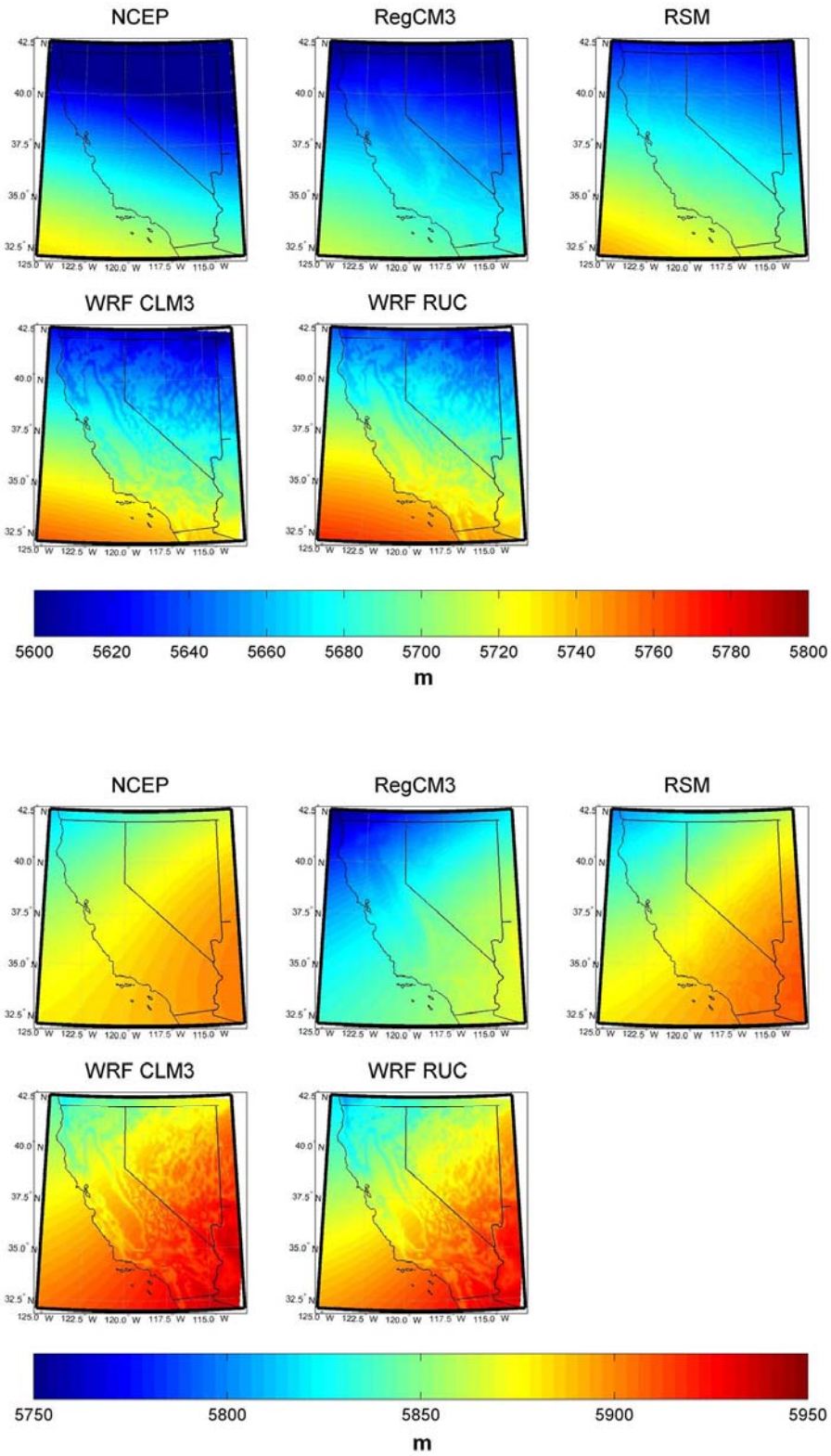

Figure 12. Geopotential height (a) January mean-monthly distribution, and (b) July mean-monthly distribution

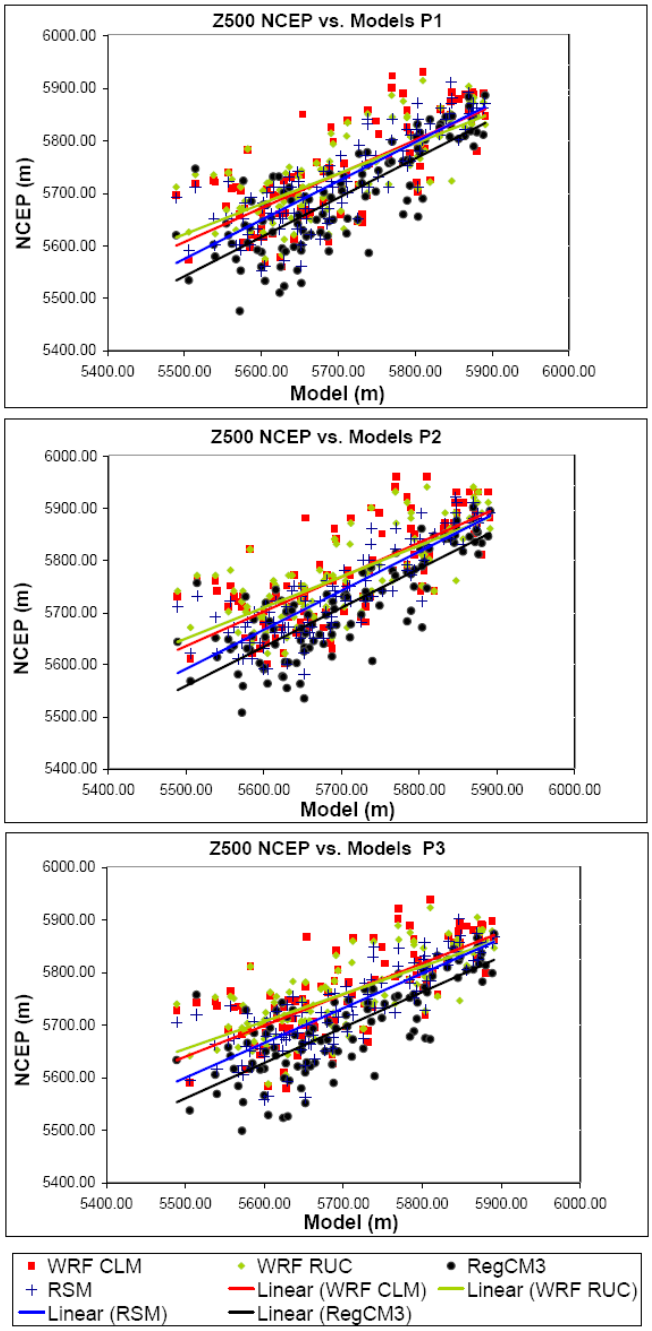

Figure 13. Model and Reanalysis comparison of the 500 hectopascal (hPa) geopotential height for three locations P1. 120W, 39N (American River Basin), P2. 117.5W, 37N (Merced Basin), and P3. 122.5W, 38N (Russian River Basin)

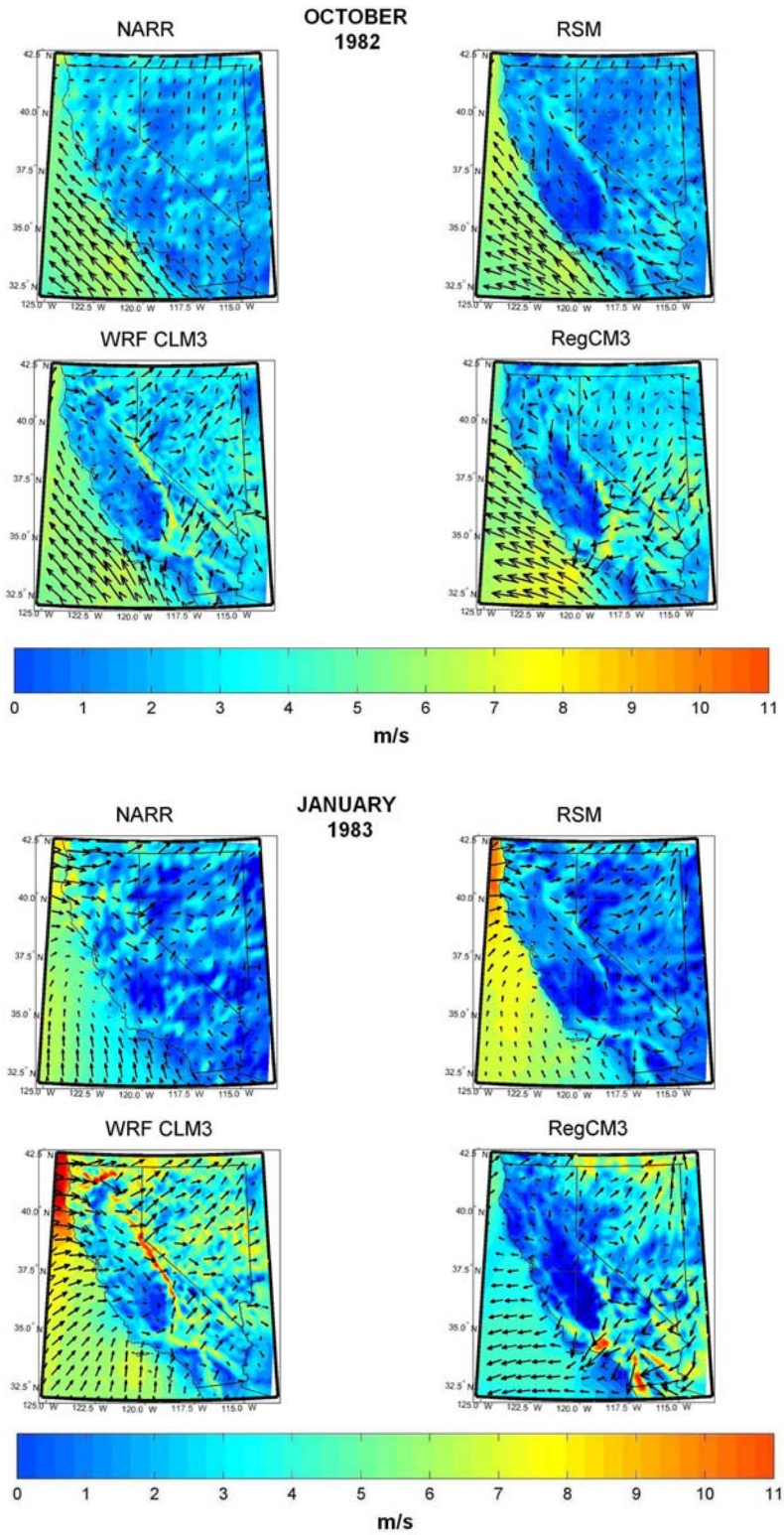

Figure 14. Model and reanalysis near-surface wind speed and direction for (a) mean-October 1982 and (b) mean-January 1983

flow in the southern region. These results are being further analyzed, along with a number of other terms, in a follow-on manuscript that is in preparation.

To understand the time-evolution of the height fields, fields that reveal the presence of storm systems propagating through the study domain. Except as noted below, the models reproduce the large-scale patterns in surface wind components estimated by NARR. However, errors in individual grid cells can be comparable in magnitude to the wind component itself. In significant regions of Southern California, RegCM3 has an incorrect sign on one or both wind components.

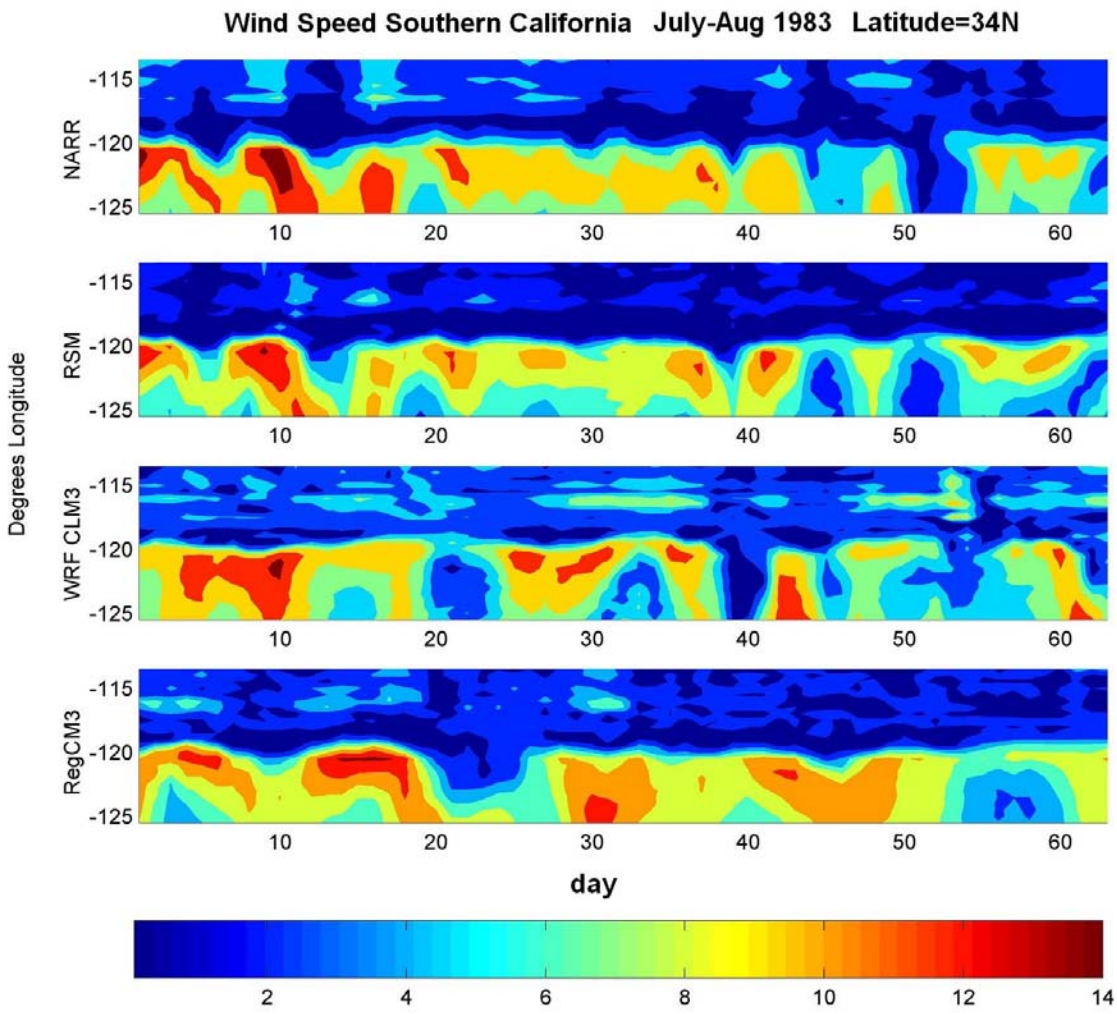

Figure 15. Hovmueller plots of the JJA wind speed and direction across latitude 38.5N. The legend along the bottom is wind speed in meters per second.

The wind speed and direction plots show in Figure 15 provide more details on the structure of the low boundary wind along the coastal interface, an important impact zone that has yet to be well evaluated. Here we show the time-evolving July through August 1983 strengthening of the summer wind as in flows along shore and weakens. In each model the offshore winds are near 14 meter per hour, with RSM following the NARR reanalysis closest. Each model well captures the weakening as the winds arrive onshore. Again, this part of the analysis is preliminary and a more comprehensive study is being prepared as part of a separate report. As a further analysis of the model-simulated heights, we have added 1980–1989 precipitation Hovmeuller plots for Northern California and the Pacific Ocean at latitude 38.5 for longitudes
-119 to -123, including the Russian and American River Basins. Figure 16 shows these results using PRISM, CANA, RSM, RegCM3, WRF-CLM3, and WRF-RUC. Precipitation making landfall is near -122 and shows good skill using CANA, WRF-CLM3, and RSM, but is overestimated by RegCM and WRF-RUC. The American River Basin is closer to Longitude -123, where WRF-CLM3 shows the highest overall skill for this location.

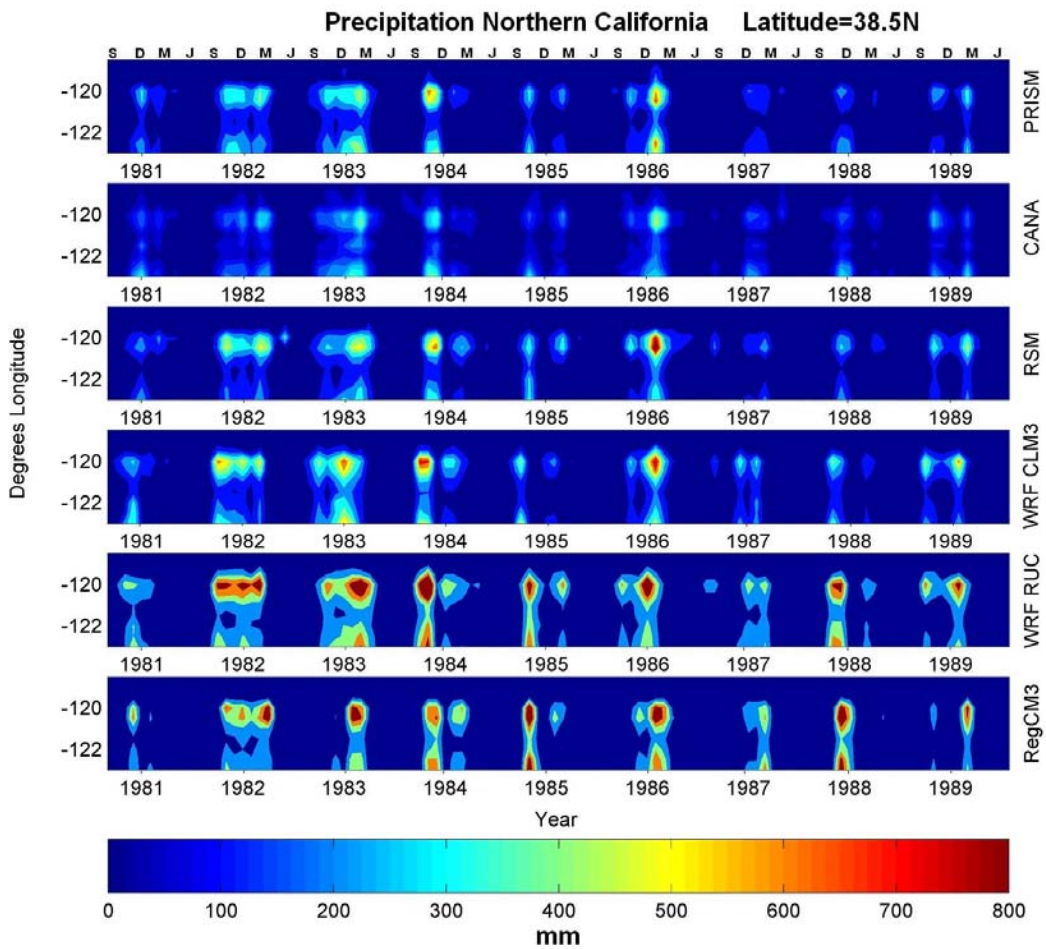

Figure 16. Hovmueller plots of the winter precipitation across latitude 38.5N

4.0 Summary and Conclusions

Any downscaling approach is only as good as the large-scale forcing used. This study used reanalysis initial and boundary conditions to isolate shortcomings in the downscaling methods. To further isolate the effects of different model formulations, the three dynamic downscaling models (WRF-CLM3, RegCM3, and RSM) that we ran and analyzed were configured with domains and grid spacing as close as possible to identical. Unique to each model are the parameterization schemes for boundary layer development, cloud physics, convection, and land surface processes. More important is the boundary condition updating method. The lateral boundary conditions differ most significantly between the spectral model (RSM) and the Cartesian models (RegCM3, WRF-CLM3). Spectral updating is a fully internal procedure, where the large-scale values update the entire field, while latitude-longitude model updates are along a set of nudge points based on the Barnes (1973) or Cressman (1959) schemes. This difference is important for the way in which the internal dynamics sets up, and the degree of independence the RCMs have within the internal fields. Error propagation using the spectral approach may likely be more damped, and when evaluating with the large-scale signals are better behaved.

As noted in detail above, all the models (dynamical and statistical) analyzed here have limitations. Nonetheless, they perform as well as other state-of-the-art downscaling systems, and all do a credible job simulating the historical climate of California. The empirically based CANA statistical approach is based on historical observations and hence, when compared for this period performs at least as well as the dynamical models. Its errors tend to be distinct from those of the dynamical models. The most important limitation of this approach is the very limited set of output variables (near-surface temperature and precipitation) that have so far been predicted using this method. There is no fundamental reason why additional meteorological quantities could not be simulated using this approach.

The dynamical models do better at simulating the large-scale circulation (as diagnosed by 500 mb heights), surface winds, and near-surface temperatures than parameterized quantities such as clouds, precipitation, and snow cover. Errors in these quantities lead to errors in others; for example, deficiencies in cloud amounts and snow cover results in large errors on downwelling and upwelling short-wave fluxes. Snow cover is particularly difficult to simulate, being sensitive primarily to simulated meteorology, but also to land-surface processes. None of the models evaluated here simulated year-round snow cover well. Among the dynamical models, WRF-CLM3 performs best at simulating seasonal precipitation amounts.

Our archived data is being further analyzed and process level statistics will be developed to design a bias correction. Improving observations is beyond the scope of this work, but we acknowledge a need for continued effort in this area of research and measurement, and matching point and gridded data. These results will provide a benchmark to the California assessment process. It is hoped that the plots and discussion provided help to guide readers that utilize these results as part of an assessment of impacts on California due to climate change.

5.0 References

Barnes, S. L. 1973. Mesoscale objective analysis using weighted time-series observations. NOAA Tech. Memo. ERL NSSL-62. National Severe Storms Laboratory, Norman, Oklahoma 73069, 60 pp. [NTIS COM-73-10781].

CARB (California Air Resources Board). 2008. *California Air Resources Board AB 32 Climate Change Proposed Scoping Plan, Pursuant to AB32, The California Global Warming Solutions Act of 2006.* 142 pp. www.arb.ca.gov/cc/scopingplan/document/psp.pdf.

California Regional Assessment. 2002. *Preparing for a changing climate: The potential consequences of climate variability and change. California.* R. Wilkinson, K. Clarke, M. Goodchild, J. Reichman, and J. Dozier, eds. 431pp. www.ncgia.ucsb.edu/pubs/CA_Report.pdf.

California Regional Scenarios. 2006. *Scenarios of climate change in California: An overview.* A report from the California Climate Change Center. D. Cayan, A. L. Luers, M. Hanemann, G. Franco, and B. Croes. CEC-500-2005-186-SF. 53 pp.

Christensen, J. H., T. R. Carter, M. Rummukainen, and G. Amanatidis. 2007. "Evaluating the performance and utility of climate models: The PRUDENCE project." *Climatic Change* 81. doi:10.1007/s10584-006-9211-6.

Chou, M. D., and M. J. Suarez. 1994. *An efficient thermal infrared radiation parameterization for use in General Circulation Models.* Technical Report Series on Global Modeling and Data Assimilation, National Aeronautical and Space Administration/TM-1994-104606, 3:85 pp.

Chou M.-D., and M. J. Suarez. 1999. A solar radiation parameterization for atmospheric studies. NASA Tech. Memo. 1999-104606, 40 pp.

Chou, M. D., and K. T. Lee. 1996. "Parameterizations for the Absorption of Solar Radiation by Water Vapor and Ozone." *J. Atmos. Sci.* 53:1203–1208.

Cressman, G. P. 1959. "An operational objective analysis system." *Month. Wea. Rev.* 87:367–374.

Curry, J. A., and A. H. Lynch. 2002. "Comparing Arctic Regional Climate Models." *EOS* 83:87.

Daly, C., G. H. Taylor, W. P. Gibson, T. W. Parzybok, G. L. Johnson, and P. Pasteris. 2001. "High-quality spatial climate data sets for the United States and beyond." *Transactions of the American Society of Agricultural Engineers* 43:1957–1962.

Daly, C., M. Halbleib, J. I. Smith, W. P. Gibson, M. K. Doggett, G. H. Taylor, J. Curtis, and P. A. Pasteris. 2008. "Physiographically-sensitive mapping of temperature and precipitation across the conterminous United States." *International Journal of Climatology* DOI: 10.1002/joc.1688.

Daly, C., W. P. Gibson, M. Doggett, J. Smith, and G. Taylor. 2004. A probabilistic-spatial approach to the quality control of climate observations. *Proc., 14th AMS Conf. on Applied Climatology, 84th AMS Annual Meeting Combined Preprints*, Amer. Meteorological Soc., Seattle, Washington, January 13–16, 2004, Paper 7.3, CD-ROM. Presented to NRCS, 9 Mar 2005.

Davies, H. C., 1983. Limitations of some common lateral boundary schemes used in regional NWP models. *Mon. Wea. Rev.* 111:1002–1012.

Déqué, M., D. P. Rowell, D. Lüthi, F. Giorgi, J. H. Christensen, B. Rockel, D. Jacob, E. Kjellström, M. de Castro, and B. van den Hurk. 2007. "An intercomparison of regional climate simulations for Europe: Assessing uncertainties in model projections." *Climatic Change* 81. doi:10007/s10584-006-9228-x.

Dickinson, R. E., A. Henderson-Sellers, and P. J. Kennedy. 1993. Biosphere-Atmosphere Transfer Scheme (BATS) Version 1e as Coupled to the NCAR Community Climate Model. NCAR TN-387+STR, NCAR, Boulder, Colorado.

Dickinson, R. E., A. Henderson-Sellers, P. J. Kennedy, and M. F. Wilson. 1986. Biosphere-Atmosphere Transfer Scheme (BATS) for the NCAR Community Climate Model. NCAR Technical Note, NCAR, TN275+STR, 69pp.

Dudhia, J. 1989. "Numerical study of convection observed during the winter monsoon experiment using a mesoscale two-dimensional model." *J. Atmos. Sci.* 46:3077–3107.

Duffy, P. B., R. W. Arritt, J. Coquard, W. Gutowski, J. Han, J. Iorio, J. Kim, L.-R. Leung, J. Roads, and E. Zeledon. 2006. "Simulations of present and future climates in the western U.S. with four nested regional climate models." *J. Climate* 19:873–895.

Ek, M. B., K. E. Mitchell, Y. Lin, E. Rogers, P. Grunmann, V. Koren, G. Gayno, and J. D. Tarpley. 2003. "Implementation of Noah land surface model advances in the National Centers for Environmental Prediction operational mesoscale Eta model." *J. Geophys. Res.* 108(D22): 8851, doi:10.1029/2002JD003296.

Field, C. B., G. C. Daily, F. W. Davis, S. Gaines, P. A. Matson, J. Melak, and N. L. Miller. 1999. *Confronting climate change in California: Ecological impacts on the golden state.* A report of the Union of Concerned Scientists, Cambridge, Massachusetts, and the Ecological Society of America, Washington, D.C. 62pp.

Fiorino, M. 2004. A Multi-decadal Daily Sea Surface Temperature and Sea Ice Concentration Data Set for the ERA-40 Reanalysis. ERA-40 project Report Series. ECMWF, Shinfield Park, Reading, RG2 9AX, UK. 16pp.

Fritsch, J. M., and C. F. Chappell. 1980. "Numerical Prediction of Convectively Driven Mesoscale Pressure Systems. Part 1: Convective Parameterization." J*ournal of the Atmospheric Sciences* 37(8): 1722–1733.

Fu, C. B., S. Y. Wang, Z. Xiong, W. J. Gutowski, D. K. Lee, J. McGregor, Y. Sato, H. Kato, J.-W. Kim, M.-S. Su. 2005. "Regional Climate Model Intercomparison Project for Asia (RMIP)." *Bull. Amer. Meteor. Soc*.

Gates, W. L. 2003. *Modeling regional climate change in California.* California Energy Commission. P500-03-025FA1. 18 pp.

Grell, G. A. 1993. "Prognostic Evaluation of Assumptions Used by Cumulus Parameterizations." *Monthly Weather Review* 121: 764–787.

Grell, G. A., and D. Devenyi. 2002. "A generalized approach to parameterizing convection combining ensemble and data assimilation techniques." *Geoph. Res. Let*. 29(14): 10, 1029/2002GL015311, 2002.

Gutowski, W. J., G. L. Potter, and M. R. Riches. 1988. "DOE model intercomparison workshop II." *Bull. Am. Meteor. Soc*. 69: 1453–1454.

Gutowski, W. J., E. S. Takle, and R. W. Arritt. 1998. "Project to Intercompare Regional Climate Simulations - Workshop II, 5–6 June 1997." *Bull. Am. Meteor. Soc*. *79*: 657–659.

Gutowski, W. J., R. W. Arritt, E. S. Takle, Z. Pan, F. Giorgi, J. H. Christensen, S.-Y. Hong, W. M. Lapenta, G. E. Liston, J. McGregor, and J. O. Roads. 2000. "Project to Intercompare Regional Climate Simulations: Advancing the CLIVAR Agenda." *CLIVAR Exchanges* 5:13–15.

Hayhoe, K., D. Cayan, C. Field, P. C. Frumhoff, E. P. Maurer, N. L. Miller, S. C. Moser, S. H. Schneider, K. N. Cahill, E. E. Cleland, L. Dale, R. Drapek, R. M. Hanemann, L. S. Kalkstein, J. Lenihan, C. Lunch, R. P. Nielson, S. Sheridan, and J. Veriville. 2004. "Emission pathways, climate change, and impacts on California." *Proc. Nat. Acad. Sci.* 101:12422–12437.

Hidalgo, H. G., M. D. Dettinger, and D. R. Cayan. 2008. *Downscaling with Constructed Analogues: Daily Precipitation and Temperature Fields Over the United States*. California Energy Commission, PIER Energy-Related Environmental Research. CEC-500-2007-123. 48 pp. www.energy.ca.gov/2007publications/CEC-500-2007-123/CEC-500-2007-123.PDF.

Holtslag, A. A. M., and B. A. Boville. 1993. "Local Versus Nonlocal Boundary-Layer Diffusion in a Global Climate Model." *Journal of Climate* 6(10): 1825–1842.

Hong, S. Y., and H. L. Pan. 1996. "Nonlocal Boundary Layer Vertical Diffusion in a Medium-Range Forecast Model." *Mon. Wea. Rev.* 124: 2322–2339.

Hong, S.-Y., J. Dudhia, and S.-H. Chen. 2004. A Revised Approach to Ice Microphysical Processes for the Bulk Parameterization of Clouds and Precipitation. *Mon. Wea. Rev.* 132: 103–120.

Iacobellis, S. F., and R. C. J. Somerville. 2000. "Implications of Microphysics for Cloud-Radiation Parameterizations: Lessons from TOGA COARE." *J. Atmos. Sci.* 57:161–183.

Imbert, A., and R. E. Benestad. 2005. "An improvement of analog model strategy for more reliable local climate change scenarios." *Theoretical and Applied Climatology* 82(3–4). September. DOI 10.1007/s00704-005-0133-4.

IPCC (Intergovernmental Panel on Climate Change). 2001. *Climate Change 2001: The Scientific Basis. Contribution of Working Group I to the Third Assessment Report of the Intergovernmental Panel on Climate Change.* Ed. J. T. Houghton, Y. Ding, M. Griggs, D. J. Noguer, P. J. van der Linden, X. Dai, K. Maskell, and C. A. Johnson. Cambridge, UK: Cambridge University Press. 881 pp.

IPCC. 2007. *Climate Change 2007: The Physical Basis. Contribution of Working Group I to the Fourth Assessment Report of the Intergovernmental Panel on Climate Change.* Ed. S. Solomon, D. Qin, M. Manning, Z. Chen, M. Marquis, K. B. Averyt, M. Tignor, and H. L. Miller. Cambridge, UK: Cambridge University Press. 996 pp.

Jacob, D., L. Bärring, O. B. Christensen, J. H. Christensen, M. de Castro, M. Déque, F. Giorgi, S. Hagemann, M. Hirschi, R. Jones, E. Kjellström, G. Lenderink, B. Rockel, E. Sánchez, C. Schär, S. I. Seneviratne, S. Somot, A. van Ulden, and B. van den Hurk. 2007. "An inter-comparison of regional climate models for Europe: Design of the experiments and model performance." *Climatic Change* 81. doi:10007/s10584-006-9213-4.

Jin, J., N. J. Schlegel, and N. L. Miller. 2008. Analysis of Sea Surface Temperature Boundary Conditions Using the Weather Research and Forecasting Model. Spring AGU Joint Assembly, Ft. Lauderdale, Florida, 30 May 2008.

Juang, H.-M. H., and M. Kanamitsu. 1994. "The NMC nested regional spectral model." *Mon. Wea. Rev.* 122: 3–26.

Kain, J. S. 2004. "The Kain-Fritsch convective parameterization: An update." *J. Applied Meteor*. 43: 170–181.

Kanamitsu, M., and H. Kanamaru. 2007. "57-Year California Reanalysis Downscaling at 10 km (CaRD10) Part 1. System Detail and Validation with Observations." *J. Climate* 20:5527–5552.

Kanamitsu, M., H. Kanamaru, Y. Cui, and H. Juang. 2005. *Parallel Implementation of the Regional Spectral Atmospheric Model.* CEC-500-2005-014. Available from www.energy.ca.gov/2005publications/CEC-500-2005-014/CEC-500-2005-014.

Kanamaru, H., and M. Kanamitsu. 2007. "Scale-Selective Bias Correction in a Downscaling of Global Analysis using a Regional Model." *Monthly Weather Review* 135(2): 334–350.

Kiehl, J. T. et al. 1996. Description of the NCAR Community Climate Model (CCM3). NCAR TN-420+STR, CGD, NCAR.

Kueppers, L. M., M. A. Snyder, L. C. Sloan, D. Cayan, J. Jin, H. Kanamaru, M. Kanamitsu, N. L. Miller, M. Tyree, H. Du, and B. Weare. 2008. "Regional climate effects of irrigation and urbanization in the western United States: A model intercomparison." *Global and Planetary Change* 60:250–264.

Leung, L. R., S. J. Ghan, Z-C Zhao, Y. Luo, W-C Wang, and W-L Wei. 1999. Intercomparison of regional climate simulations of the 1991 summer monsoon in eastern Asia. *J. Geophys. Res.* 104: 6425–6454.

Leung, L. R., and Y. Qian. 2003. "The sensitivity of precipitation and snowpack simulations to model resolution via nesting in regions of complex terrain." *J. Hydrometeorol*. 4: 1025–1043.

Lin, Y.-L., R. D. Farley, and H. D. Orville. 1983. "Bulk parameterization of the snow field in a cloud model." *J. Climate Appl. Meteor* 22:1065–1092.

Maurer, E. P., A. W. Wood, J. C. Adam, D. P. Lettenmaier, and B. Nijssen. 2002. "A Long-Term Hydrologically Based Data Set of Land Surface Fluxes and States for the Conterminous United States." *J. Climate* 15(22): 3237–3251.

Maurer, E. P., and H. G. Hidalgo. 2008. "Utility of daily vs. monthly large-scale climate data: An intercomparison of two statistical downscaling methods." *Hydrology and Earth System Sciences* 12: 551–563.

Mearns, L. 2004. NARCCAP North American Regional Climate Change Assessment Program. A Multiple AOGCM and RCM Climate Scenario Project over North America. 12/17/2004. AGU Fall Meeting, San Francisco, USA.

Mellor, G. L., and T. Yamada. 1982. Development of a turbulence closure model for geophysical fluid problems. *Rev. Geophys. Space Phys.* 20:851–875.

Mlawer, E. J., S. J. Taubman, P. D. Brown, M. J. Iacono, and S. A. Clough. 1997. "Radiative transfer for inhomogeneous atmosphere: RRTM, a validated correlated-k model for the long-wave." *J. Geophys. Res*. 102(D14): 16663–16682.

Miller, N. L. and N. J. Schlegel, 2006. Climate projected California fire weather sensitivity: California Santa Ana wind occurrence. *Geophys. Res. Lett*. 33, L15711, doi:10.10292006GL025808.

Moorthi, S., and M. J. Suarez. 1992. "Relaxed Arakawa-Schubert: A parameterization of moist convection for general circulation models." *Mon. Wea. Rev.* 120: 978–1002.

National Research Council, 1998. Future of the National Weather Service Cooperative Observer Network. National Weather Service Modernization Committee, ISBN: 978-0-309-06146-9, 78pp.

National Weather Service, 2000. Cooperative Observer Program (COOP). U.S. Department of Commerce, National Oceanic and Atmospheric Administration, National Weather Service. http://www.coop.nws.noaa.gov.

Oleson, K. W. et al. 2004. Technical description of the community land model (CLM). NCAR Tech. Note NCAR/TN-461+STR. 186 pp.

Orville, H. D., and F. J. Kopp. 1977. Numerical simulation of a hailstorm. *J. Atmos. Sci.* 34:1596–1618.

Pal, J. S. et al. 2007. "Regional climate modeling for the developing world - The ICTP RegCM3 and RegCNET." *Bulletin of the American Meteorological Society* 88:1395–1409.

Pan, Z., J. H. Christensen, R. W. Arritt, W. J. Gutowski, Jr., E. S. Takle, and F. Otieno. 2001. "Evaluation of uncertainties in regional climate change simulations." *J. Geophys. Res*. 106: 17,735–17,752.

Pan, H.-L., and L. Mahrt. 1987. "Interaction between soil hydrology and boundary layer developments." *Boundary-Layer Meteor.* 38: 185–202.

Slater, A. G., C. A. Schlosser, C. E. Desborough, A. J. Pitman, A. Henderson- Sellers, A. Robock, K. Ya. Vinnikov, K. Mitchell, A. Boone, H. Braden, F. Chen, P. Cox, P. de Rosnay, R. E. Dickinson, Y-J. Dai, Q. Duan, J. Entin, P. Etchevers, N. Gedney, Ye. M. Gusev, F. Habets, J. Kim, V. Koren, E. Kowalczyk, O. N. Nasonova, J. Noilhan, J. Shaake, A. B. Shmakin, T. Smirnova, D. Verseghy, P. Wetzel , Y. Xue, Z-L. Yang. 2001. "The representation of snow in land-surface schemes: Results from PILPS 2(d)." *J. Hydrometeorology* 2:7–25.

Shimpo, A., and M. Kanamitsu. 2008. Comparison of Four Cloud Schemes in Simulating the Seasonal Mean Field Forced by the Observed Sea Surface Temperature. In print, *Mon. Wea. Rev.*

Skamarock, W. C., J. B. Klemp, J. Dudhia, D. O. Gill, D. M. Barker, W. Wang, and J. G. Powers. 2005. A Description of the Advanced Research WRF Version 2, NCAR Tech Note, NCAR/TN–468+STR, 88 pp.

Snyder, M. A., L. M. Kueppers, L. C. Sloan, D. Cayan, J. Jin, H. Kanamaru, M. Kanamitsu, N. L. Miller, M. Tyree, H. Du, and B. Weare. 2006. Regional climate effects of irrigation and urbanization in the western United States: A model intercomparison. CEC-5000-2006-031, 43pp.

Takle, E. S., W. J. Gutowski, R. A. Arritt, Z. Pan, C. J. Anderson, R. R. da Silva, D. Cayan, S.-C. Chen, J. H. Christensen, S.-Y. Hong, H.-M. H. Juang, J. Katzfey, W. M. Lapenta, R. Laprise, P. Lopez, J. McGregor, and J. O. Roads. 1999. "Project to Intercompare Regional Climate Simulations (PIRCS): Description and initial results." *J. Geophys. Res*. 104:19,443–19,461.

Taylor, K. E. 2001. "Summarizing multiple aspects of model performance in single diagram." *J. Geophys. Res.* 106:(D7): 7183–7192.

Taylor, K. E., D. Williamson, and F. Zwiers. 2000. *The sea surface temperature and sea-ice concentration boundary conditions of AMIP II simulations.* PCMDI report #60, 20 pp.

Tiedtke, M. 1993. "Representation of Clouds in Large-Scale Models." Mon. Wea. Rev. 121: 3040–3061.

USGCRP. 2001. National Assessment Synthesis Team, Climate Change Impacts on the United States: The Potential Consequences of Climate Variability and Change. U.S. Global Change Research Program. Cambridge, UK: Cambridge Press. 154 pp.

Wilby, R. L., and T. M. L. Wigley. 2000. "Precipitation predictors for downscaling: Observed and general circulation model relationships." *International Journal of Climatology* 20: 641–661.

Wood, A. W., L. R. Leung, V. Sridhar, and D. P. Lettenmaier. 2004. "Hydrologic implications of dynamical and statistical approaches to downscaling climate model outputs." *Climatic* Change 62: 189–216.

Yoshimura, K., and M. Kanamitsu. 2008. Specification of External Forcing for Regional Model Integrations. In print. *Mon. Wea. Rev.*

Zorita, E., and H. von Storch. 1999. "The Analog Method as a Simple Statistical Downscaling Technique: Comparison with More Complicated Methods." *J. Climate* 12:2474–2489. DOI: 10.1175/1520-0442(1999)012<2474:TAMAAS>2.0.CO;2.